IMPROVED APPROXIMATIONS FOR THE PERIMETER OF AN ELLIPSE

MIKA INKI

Abstract. We give three closed formulas, with three, four and six square roots, for the perimeter P of an ellipse with semi-axes $a \geq b \geq 0$. In exact arithmetic their maximum relative errors over all eccentricities, 4.0×10^{-8}, 4.1×10^{-17} and 8.1×10^{-37}, lie below the unit roundoff of single, double and quadruple precision, respectively, and evaluated in that precision they are accurate to within about six units of it (for quadruple precision, as estimated with 34-digit decimal arithmetic). Each formula writes a fixed number of steps of the arithmetic–geometric mean (AGM) as one expression, in a form that avoids the harmful cancellation. For flat ellipses, where any fixed number of AGM steps eventually fails (as $b \to 0$ it tends to $2\pi a$ instead of $4a$), it switches to an approximation based on Legendre's relation, which expresses the complete elliptic integral E of the second kind exactly through the integral K of the first kind and two power series in b/a: the AGM steps supply an estimate of K, and the series are truncated to short polynomials. A final term makes the formula continuous at the switch, and we give the range of its coefficient that suffices for each precision. We prove that for every switch point and every accuracy there are such continuous formulas, and that the error of the continuous formula is at most that of the AGM branch plus twice that of the flat-ellipse branch. The formulas are exact at $b = 0$ and at $b = a$; numerically, they are increasing in b and more accurate than Ramanujan's second approximation at every eccentricity, by factors of at least 289, 2.8×10^{11} and 4.1×10^{32}. With the latency of three, four or six AGM steps, they are faster than an AGM loop of the same accuracy for flat ellipses, where the loop needs more steps.

We also study nested-radical generalisations $P \approx \pi(a+b)(1+3h/D)$ of Ramanujan's second approximation, with $h = ((a-b)/(a+b))^2$ and D a constant plus nested square roots of a polynomial in h. Ramanujan's formula is a degenerate member of a one-parameter family of double-nested forms that agree with the Gauss–Kummer series through h^4. We derive double- and triple-nested formulas with integer coefficients and double-, triple- and quadruple-nested formulas with real coefficients: formulas that are, as verified numerically, nowhere less accurate than Ramanujan's, formulas that agree with the series to the highest order possible for their depth, and minimax formulas. The best of them reduce the maximum error of Ramanujan's formula by up to five orders of magnitude. We also give a numerically stable evaluation in powers of $1 - h$, tabulate the errors of all formulas at seven eccentricities where the perimeter has a closed form, and compare their cost with that of the AGM in double and single precision.

hexagon:2611.01145v1

1. Introduction

The perimeter of an ellipse with semi-axes $a \geq b \geq 0$ and eccentricity $e = \sqrt{1 - b^2/a^2}$ is

$$P = 4a \int_0^{\pi/2} \sqrt{1 - e^2 \sin^2\theta}\, d\theta = 4a\, E(e), \tag{1}$$

where E is the complete elliptic integral of the second kind. Unlike the area πab, the perimeter has no expression in terms of elementary functions, and the search for simple and accurate approximations has a long history; see the reviews by Sýkora [29, 30] and the survey of Almkvist and Berndt [3]. The best-known approximations are the two given by Ramanujan in 1914 [25],

$$R_{\mathrm{I}} = \pi\Big(3(a+b) - \sqrt{(3a+b)(a+3b)}\Big), \tag{2}$$

$$R_{\mathrm{II}} = \pi(a+b)\Big(1 + \frac{3h}{10 + \sqrt{4-3h}}\Big), \qquad h = \Big(\frac{a-b}{a+b}\Big)^2. \tag{3}$$

Date: November 2026.

2020 *Mathematics Subject Classification.* Primary 33E05; Secondary 41A50, 65D20, 51M25.

Key words and phrases. Perimeter of an ellipse, complete elliptic integrals, arithmetic–geometric mean, Legendre's relation, Ramanujan's approximations, Gauss–Kummer series, nested radicals, minimax approximation.

The second one is remarkably accurate: its relative error is $O(h^5)$ as $h \to 0$, and its largest value, about 4.0×10^{-4}, occurs for the degenerate ellipse $b = 0$; see Villarino [31] and Barnard, Pearce and Schovanec [7] for sharp error bounds of this type. The question of why the perimeter has no simple formula, and how good the known approximations are, has also reached a wide audience through popular presentations, for instance the Stand-up Maths video *Why is there no equation for the perimeter of an ellipse?* [28].

For $b > 0$ the perimeter can also be computed to any accuracy with the arithmetic–geometric mean (AGM) [8, 26]. The AGM eventually converges quadratically, but it is an iteration: the number of steps needed grows without bound as the ellipse becomes flatter, and every truncation of it fails completely as $b \to 0$.

Recent work has refined Ramanujan's second approximation by symbolic regression [23], by an exponential correction factor [4] and by a correction of its radicand [27], and has proposed other closed forms that combine rational functions with logarithms [5]; the most accurate of these closed formulas, the ELIP family of Ayala-Raggi and Rendón-Marín [5], reaches a certified maximum relative error of 4.5×10^{-10}. For numerical libraries, Hastings [18] and Cody [13] gave approximations of E of the form $p_1(\eta) + p_2(\eta)\ln(1/\eta)$ with polynomials p_1 and p_2 in $\eta = (b/a)^2$, the latter with maximum errors down to 3.8×10^{-18}, and Fukushima [15, 16, 17] developed piecewise polynomial and rational approximations accurate to within a few machine epsilons in single and double precision. These approximations need a logarithm and coefficients computed separately for each precision, and the piecewise ones are continuous only to within their approximation error.

Our main results (Section 3) are three closed formulas built from a fixed number of AGM steps, written as one expression in a form that avoids the harmful cancellation. For flat ellipses, where any fixed number of AGM steps eventually fails, they switch to an approximation based on Legendre's relation, which expresses E exactly through the complete elliptic integral K of the first kind and two power series in $t = b/a$; the series are truncated, and K is estimated from the same AGM steps. A single extra term makes the two branches agree at the switch. In exact arithmetic, the resulting formulas have maximum relative errors below the unit roundoff of single, double and quadruple precision:

- A_3 (three square roots): maximum relative error 4.0×10^{-8}, below $2^{-24} \approx 6.0 \times 10^{-8}$;
- A_4 (four square roots): maximum relative error 4.1×10^{-17}, below $2^{-53} \approx 1.1 \times 10^{-16}$;
- A_6 (six square roots): maximum relative error 8.1×10^{-37}, below $2^{-113} \approx 9.6 \times 10^{-35}$,

in each case for all eccentricities $0 \le e \le 1$, including the degenerate ellipse $b = 0$, where they give exactly $4a$. Evaluated in binary32 and binary64, A_3 and A_4 are accurate to within about six units of the unit roundoff, and emulated 34-digit decimal arithmetic suggests that A_6 is accurate to within a few units in binary128. The formulas are continuous, contain no loops, and use a single comparison to choose between two branches of almost equal latency; numerically, they are increasing in b and more accurate than Ramanujan's second approximation at every eccentricity, by factors of at least 289, 2.8×10^{11} and 4.1×10^{32}. In double precision, A_4 has about the latency of four AGM steps, whereas an AGM loop iterated to the same accuracy needs, in exact arithmetic, more steps for $b/a < 0.09$ (and fewer for $b/a > 0.55$), and ever more as $b \to 0$; in binary64 the loop moreover loses accuracy for flat ellipses (Section 13.1). The continuity coefficient may vary in a wide interval without the error or the jump at the switch exceeding the unit roundoff, and for A_4 and A_6 it may even be omitted, at the price of a jump below the unit roundoff (Table 1). Unlike the recent closed formulas cited above, whose maximum errors are at least 4.5×10^{-10}, A_4 and A_6 are accurate to double and quadruple precision, and unlike the library approximations, all three formulas need no logarithm: they use only arithmetic operations and square roots, which IEEE 754 requires to be correctly rounded [19], use a single small set of exact coefficients for all shapes and contain no fitted parameters, and the same construction gives a continuous formula for any precision (Proposition 4.1).

The second part of the note (Sections 6–10) keeps the structure of Ramanujan's second approximation (3) and replaces its square root $\sqrt{4 - 3h}$ by nested square roots of polynomials in h, a form that, to our knowledge, has not been considered before. The resulting short, branch-free formulas reduce the maximum error of R_{II} by up to five orders of magnitude. The analysis also

clarifies Ramanujan's formula: R_{II} is the degenerate member, with a perfect-square inner radicand, of a one-parameter family of double-nested forms that all agree with the Gauss–Kummer series through h^4, and its accuracy near the circle comes from two vanishing coefficients in an ideal radicand (Section 2). We consider four families, with double-, triple- and, except for the integer formulas, quadruple-nested members:

(1) integer-coefficient formulas that are, as verified numerically, nowhere less accurate than R_{II} (Section 7),
(2) real-coefficient formulas with the same property, numerically optimised for the smallest maximum error (Section 8),
(3) formulas that agree with the Gauss–Kummer series to the highest order possible for their depth (Section 9),
(4) minimax formulas, numerically optimised for the smallest maximum error without further constraints (Section 10).

Section 2 collects background, Sections 3–5 state, derive and analyse the main formulas, and Section 6.5 gives a numerically stable evaluation of the nested-radical formulas. Section 11 lists seven eccentricities with closed-form perimeters and the errors of all formulas there, and Sections 12 and 13 summarise the accuracy and the cost of all formulas and explain how the cost was estimated, in double and in single precision.

All results in this note were derived with the assistance of the large language model Claude Opus 5.5 (Anthropic), which carried out the derivations and the searches, numerical optimisation and high-precision verification described in Section 14; see also the provenance statement at the end.

2. Preliminaries

2.1. **The Gauss–Kummer series.** Write $\lambda = (a-b)/(a+b)$ and $h = \lambda^2$. Parametrising the ellipse as $z(\theta) = a\cos\theta + \mathrm{i}\,b\sin\theta = \frac{a+b}{2}e^{\mathrm{i}\theta} + \frac{a-b}{2}e^{-\mathrm{i}\theta}$ gives $|z'(\theta)| = \frac{a+b}{2}\,|1-\lambda e^{-2\mathrm{i}\theta}|$, hence

$$P = \frac{a+b}{2}\int_0^{2\pi} (1-\lambda e^{-2\mathrm{i}\theta})^{1/2}(1-\lambda e^{2\mathrm{i}\theta})^{1/2}\,d\theta.$$

Expanding both factors by the binomial theorem and integrating term by term, only the diagonal terms survive, and

$$P = \pi(a+b)\,\mathcal{F}(h), \qquad \mathcal{F}(h) = \sum_{n=0}^{\infty}\binom{1/2}{n}^2 h^n = {}_2F_1\!\left(-\tfrac12,-\tfrac12;1;h\right), \tag{4}$$
$$\mathcal{F}(h) = 1 + \frac{h}{4} + \frac{h^2}{64} + \frac{h^3}{256} + \frac{25h^4}{16384} + \frac{49h^5}{65536} + \cdots.$$

This series is due to Ivory [20] and, in hypergeometric form, to Gauss and Kummer [22]; see [3] for the history. It converges for $0 \le h \le 1$, but slowly near $h = 1$, where $\mathcal{F}(1) = 4/\pi$ and $\mathcal{F}$ has a logarithmic singularity of the form $(1-h)^2\log(1-h)$.

2.2. **Normalisation.** Since $P/(\pi(a+b))$ depends only on the shape of the ellipse, every approximation in this note can be written in the form $P \approx \pi(a+b)R(h)$ (for the main formulas of Section 3, which use $t = b/a$, this is only a change of variables), and we measure it by the relative error

$$\varepsilon(h) = \frac{R(h)}{\mathcal{F}(h)} - 1,$$

which depends on the shape of the ellipse only. The variable h runs from 0 (circle) to 1 (the degenerate ellipse $b = 0$); for orientation, $e = 0.9$, 0.99 and 0.999 correspond to $h \approx 0.154$, 0.567 and 0.836. Since $\mathcal{F}(h) = 1 + h/4 + O(h^2)$, it is convenient to write

$$\mathcal{F}(h) = 1 + \frac{3h}{12\,G(h)}, \qquad 12\,G(h) = \frac{3h}{\mathcal{F}(h)-1} = 12 - \frac{3h}{4} - \frac{9h^2}{64} - \frac{27h^3}{512} - \frac{423h^4}{16384} - \cdots, \tag{5}$$

so that an approximation $R(h) = 1 + 3h/D(h)$ is exact precisely when $D = 12G$.

2.3. **Ramanujan's approximations.** In this notation R_{I} corresponds to $R(h) = 3 - \sqrt{4-h}$ and R_{II} to $D(h) = 10 + \sqrt{4-3h}$. Expanding,

$$\varepsilon_{\mathrm{I}}(h) = -\frac{h^3}{512} + O(h^4), \qquad \varepsilon_{\mathrm{II}}(h) = -\frac{3h^5}{131072} + O(h^6).$$

The high order of agreement of R_{II} with the series has a simple explanation. The function that would make D exact is $D = 10 + \sqrt{T(h)}$ with

$$T(h) = \bigl(12G(h) - 10\bigr)^2 = 4 - 3h + 0\cdot h^2 + 0\cdot h^3 - \frac{9}{2048}h^4 + O(h^5), \tag{6}$$

and the coefficients of h^2 and h^3 happen to vanish. Ramanujan's $\sqrt{4-3h}$ is therefore the square root of the first two terms of a series that is correct through h^3, and the first error comes from the neglected h^4 term of T. Shankar [27], who obtains R_{I} and R_{II} from a continued-fraction expansion of the series (Viscovatov's algorithm; see [6]), proposes the radicand $4 - 3h - \frac{9}{2048}h^4$, that is, (6) truncated after h^4.

2.4. **The arithmetic–geometric mean.** For $b > 0$ the perimeter can be computed to any precision with the Gauss–Legendre form of the AGM [8, 26]: with $a_0 = a$, $b_0 = b$, $c_0^2 = a^2 - b^2$ and

$$a_{j+1} = \tfrac{1}{2}(a_j + b_j), \qquad b_{j+1} = \sqrt{a_j b_j}, \qquad c_{j+1} = \tfrac{1}{2}(a_j - b_j),$$

one has

$$P = \frac{2\pi}{M}\Bigl(a^2 - \sum_{j\ge 0} 2^{j-1} c_j^2\Bigr), \qquad M = \lim_{j\to\infty} a_j = \lim_{j\to\infty} b_j. \tag{7}$$

Truncating after N steps and replacing M by $(a_N + b_N)/2$ gives an error that decreases quadratically once a_j/b_j is close to 1, each step roughly squaring it. For flat ellipses this phase begins only after about $\log_2 \ln(4a/b)$ steps, so the number of steps needed grows, slowly but without bound, as $b \to 0$; to reach the double-precision unit roundoff in exact arithmetic, $N = 4$ steps suffice for $e \le 0.995$ and $N = 7$ for $b/a \ge 10^{-6}$ (Section 13.1). At $b = 0$ one has $M = 0$, the formula (7) breaks down, and every truncation gives $2\pi a$ instead of $4a$ (Section 4.2). Each step costs one square root. The AGM is the basis of the main formulas of Section 3. It is also the reference method of this note, and its cost at matching accuracy is the yardstick for the cost of the closed-form approximations (Section 13).

3. Main results

Our main results are three closed formulas, A_3, A_4 and A_6, for single, double and quadruple precision. Each is built from a fixed number N of steps of the AGM, written as one expression, and has two branches. For $b \ge t_s a$ it is the truncated AGM in a form that avoids the harmful cancellation. For flat ellipses, $b < t_s a$, it is a truncated expansion obtained from Legendre's relation, in which the same AGM steps supply an estimate of the complete elliptic integral $K(e)$ of the first kind. A final term $\gamma\, t^{2n+2}$ makes the two branches agree at the switch. The derivation is given in Section 4.

Let $a \ge b \ge 0$ with $a > 0$, let $t = b/a$, and let

$$b_1 = \sqrt{ab}, \qquad a_1 = \frac{a+b}{2}, \qquad c_1 = \frac{a-b}{2},$$
$$a_{j+1} = \frac{a_j + b_j}{2}, \qquad b_{j+1} = \sqrt{a_j b_j} \qquad (j = 1, \dots, N-1).$$

Let $\mathcal{P}_n$ and $\mathcal{Q}_n$ be the polynomials obtained by truncating the series

$$\begin{aligned} \mathcal{P}(t) &= \tfrac{1}{2}t^2 + \tfrac{1}{16}t^4 + \tfrac{1}{32}t^6 + \tfrac{41}{2048}t^8 + \tfrac{59}{4096}t^{10} + \tfrac{727}{65536}t^{12} + \tfrac{1171}{131072}t^{14} + \cdots, \\ \mathcal{Q}(t) &= 1 - \tfrac{1}{4}t^2 - \tfrac{5}{64}t^4 - \tfrac{11}{256}t^6 - \tfrac{469}{16384}t^8 - \tfrac{1379}{65536}t^{10} - \tfrac{17223}{1048576}t^{12} - \tfrac{56001}{4194304}t^{14} - \cdots \end{aligned} \tag{8}$$

after the term in t^{2n}. The series are the expansions of $1 - E(t)/K(t)$ and $\pi/(2K(t))$ in powers of t, where $E(t)$ and $K(t)$ are the complete elliptic integrals with modulus t (Section 4.3). In

the formulas below, K without an argument denotes an estimate of $K(e)$ computed from the AGM steps. The single-precision formula, with three square roots, is

$$A_3: \qquad P \approx \begin{cases} \dfrac{4\pi}{a_3+b_3}\Big[a_2^2+\dfrac{b_1c_1^2}{b_2+b_1}\Big], & b \ge 0.1\,a, \\ 4a\Big[1+\dfrac{t^2}{2}\Big(K-\dfrac{1}{2}\Big)+\dfrac{t^4}{16}\Big(K-\dfrac{5}{4}\Big)+\gamma\,t^6\Big], \quad K=\dfrac{\pi a}{a_3+b_3}, & b < 0.1\,a, \end{cases} \tag{9}$$

with $\gamma = 0.1136228983147862$; the bracket on the second line is $K\mathcal{P}_2(t)+\mathcal{Q}_2(t)+\gamma\,t^6$. The double-precision formula, with four square roots, is

$$A_4: \qquad P \approx \begin{cases} \dfrac{4\pi}{a_4+b_4}\Big[a_2^2+\dfrac{b_1c_1^2}{b_2+b_1}-2(a_3-b_3)^2\Big], & b \ge 0.1\,a, \\ 4a\Big[K\,\mathcal{P}_7(t)+\mathcal{Q}_7(t)+\gamma\,t^{16}\Big], \quad K=\dfrac{4\pi a\,(a_4+b_4)}{3a_4^2+10a_4b_4+3b_4^2}, & b < 0.1\,a, \end{cases} \tag{10}$$

with $\gamma = 0.4317358822607176$. For the quadruple-precision formula, with six square roots, let

$$N_6 = a_2^2+\frac{b_1c_1^2}{b_2+b_1}-2(a_3-b_3)^2-4(a_4-b_4)^2-8(a_5-b_5)^2;$$

then

$$A_6: \qquad P \approx \begin{cases} \dfrac{4\pi N_6}{a_6+b_6}, & b \ge 0.0033\,a, \\ 4a\Big[K\,\mathcal{P}_6(t)+\mathcal{Q}_6(t)+\gamma\,t^{14}\Big], \quad K=\dfrac{4\pi a\,(a_6+b_6)}{3a_6^2+10a_6b_6+3b_6^2}, & b < 0.0033\,a, \end{cases} \tag{11}$$

with $\gamma = 0.09481603685489218$. In all three, $\mathcal{P}_n$ and $\mathcal{Q}_n$ are best evaluated by Horner's rule in t^2.

TABLE 1. The main formulas (9)–(11). N: AGM steps (square roots); n: degree of $\mathcal{P}_n$ and $\mathcal{Q}_n$ in t^2; K: estimate of $K(e)$, either $\pi a/(a_N+b_N)$ (simple) or the refined estimate (16); t_s: switch point b/a; γ: continuity coefficient (18); sufficient γ: interval for which both the maximum error in exact arithmetic and the jump at the switch stay within the unit roundoff u of the target format; error: maximum relative error over $0 \le b \le a$, in exact arithmetic and in the target arithmetic (on about 5000 shapes; a denser sample gives 3.6e−7 for A_3 and 7.1e−16 for A_4; for A_6, 34-digit decimal arithmetic; see Section 5); gain: minimum of $|\varepsilon_{\mathrm{II}}|/|\varepsilon|$ over $0 < e \le 1$, determined numerically; lat.: latency in cycles in the double-precision model (67 cycles for A_3 in the binary32 model, Section 13.2).

	target (u)	N	n	K	t_s	γ	sufficient γ	error (exact)	error (target)	gain	lat.
A_3	binary32 (6.0e−8)	3	2	simple	0.1	0.1136229	[0.0531, 0.1336]	4.0e−8	2.7e−7	289	81
A_4	binary64 (1.1e−16)	4	7	refined	0.1	0.4317359	[−0.696, 1.146]	4.1e−17	5.6e−16	2.8e11	101
A_6	binary128 (9.6e−35)	6	6	refined	0.0033	0.0948160	[−5.207, 5.359]	8.1e−37	1.5e−33	4.1e32	141

Table 1 summarises the properties of the three formulas. All three are continuous, and in exact arithmetic they are increasing in b, as is the exact perimeter (checked numerically for $10^{-12} \le b/a \le 1$). They give exactly $4a$ at $b = 0$, and $2\pi a$ at $b = a$. Their maximum relative errors in exact arithmetic, 4.0×10^{-8}, 4.1×10^{-17} and 8.1×10^{-37}, lie below the unit roundoff u of binary32, binary64 and binary128, respectively. These maxima are attained at the switch points, and the formulas are much more accurate away from them (Figure 1). Numerically, at every eccentricity they are more accurate than Ramanujan's second approximation, by factors of at least 289, 2.8×10^{11} and 4.1×10^{32}. In the target arithmetic, rounding dominates, and the errors are up to about six units of u (for A_6 as estimated with 34-digit decimal arithmetic; Section 5). Neither branch contains a loop, and the two branches have almost the same latency, although the flat branch needs more multiply–adds. In the latency model of Section 13 the formulas take about 81, 101 and 141 cycles in double precision, compared with 62 cycles for

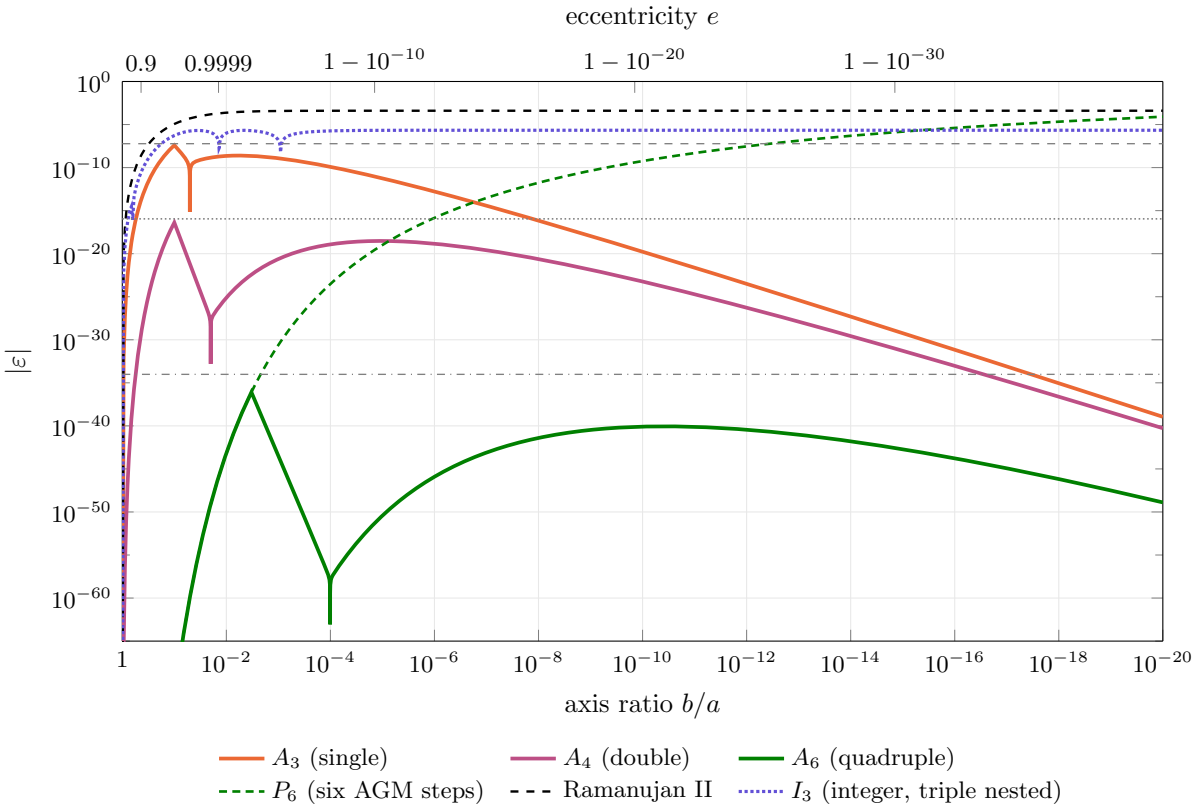

FIGURE 1. Absolute relative error $|\varepsilon|$, computed in 90-digit arithmetic, of the main formulas A_3, A_4 and A_6 (labelled with their target precisions), compared with the six-step AGM P_6 of (14) without correction for flat ellipses, with Ramanujan's second approximation R_{II}, and with the integer-coefficient triple-nested formula I_3 of Section 7, for axis ratios b/a from 1 down to 10^{-20}; errors below 10^{-65}, such as those of A_6 and P_6 for $b/a > 0.07$, lie below the plotted range. The dashed, dotted and dash-dotted grey lines mark the unit roundoff of binary32, binary64 and binary128. Each of A_3, A_4, A_6 is continuous and attains its maximum error at its switch point, $b/a = 0.1$, 0.1 and 0.0033; all three give exactly $4a$ at $b = 0$. The sharp downward spikes below the switch points, at $b/a \approx 0.050$, 0.020 and 1.0×10^{-4}, are the sign changes of their errors, which are positive for larger and negative for smaller b/a; the sampling is refined there. The three dips of I_3, at $b/a \approx 0.63$, 0.014 and 9.1×10^{-4}, are sign changes of its own error. For $b \geq 0.0033a$, A_6 coincides with P_6, whose error grows without the correction to 1.5×10^{-16} at $b/a = 10^{-6}$ and to 0.57 at $b = 0$. For $b/a \leq 10^{-6}$ the errors of R_{II} and I_3 are close to their values for the degenerate ellipse.

R_{II}, 110 for the triple-nested formula I_3 of Section 7, and 161 for seven AGM steps, the fixed number needed, in exact arithmetic, to reach double precision for all $b/a \geq 10^{-6}$. Section 5 also compares them with an AGM loop that stops as soon as it is accurate.

The continuity coefficient γ need not be stored to many digits. For a target format with unit roundoff u we call γ *sufficient* if the maximum relative error in exact arithmetic is at most u and the jump at the switch is at most u. The sufficient values form an interval (Section 4.4), and these intervals are wide. For A_3 the jump without the continuity term would be 1.1×10^{-7}, about $1.9u$ in binary32. Here the term is necessary, but any $\gamma \in [0.0531, 0.1336]$ will do, for instance $\gamma = 0.1$. For A_4 and A_6 the jumps without it, 4.2×10^{-17} ($0.38u$ in binary64) and 1.7×10^{-36} ($0.018u$ in binary128), are already below the unit roundoff. There $\gamma = 0$ is sufficient, and the term only removes the jump. Any $\gamma \in [-0.696, 1.146]$ for A_4, and any $\gamma \in [-5.207, 5.359]$ for

A_6, keeps both the maximum error and the jump within u. With γ rounded to the digits printed in (9)–(11), the remaining jumps are below 10^{-22}, 10^{-32} and 10^{-52} relative to P.

4. Derivation of the main formulas

The AGM (7) truncated after a fixed number N of steps is itself a closed formula. It has N square roots, nested N deep, and no branches. Writing several steps as one makes this explicit (Section 4.1). Every truncated AGM fails as $b \to 0$ (Section 4.2). An approximation based on Legendre's relation, which rewrites E exactly, repairs this (Section 4.3), and one further term makes the result continuous (Section 4.4).

4.1. **Several steps at once.** Let $x = \sqrt{a}$, $y = \sqrt{b}$, and let

$$\mu_1 = \frac{x+y}{2}, \qquad \mu_0 = \sqrt{xy}, \qquad \mu_2 = \sqrt{\frac{x^2+y^2}{2}}$$

be the arithmetic, geometric and quadratic means of x and y. Two steps of the AGM give

$$a_2 = \mu_1^2, \qquad b_2 = \mu_2\mu_0, \qquad c_2 = \left(\frac{x-y}{2}\right)^2,$$

and the moduli $\lambda_j = c_j/a_j$ after one and two steps are

$$\lambda_1 = \frac{a-b}{a+b} = \lambda, \qquad \sqrt{\lambda_2} = \frac{\sqrt{a}-\sqrt{b}}{\sqrt{a}+\sqrt{b}} = \frac{1-\sqrt{t}}{1+\sqrt{t}}.$$

Thus the variable $h = \lambda^2$ of the Gauss–Kummer series is the squared modulus after one AGM step, and two steps form the Borweins' quartic iteration [8]. Three steps give the closed form

$$P_3 = \frac{4\pi\mu_1^2\left(\mu_2^2 + 4\mu_2\mu_0 - 3\mu_0^2\right)}{\left(\mu_1 + \sqrt{\mu_2\mu_0}\right)^2},$$

whose relative error is 3×10^{-16} at $e = 0.85$, 1.7×10^{-14} at $e = 0.9$ and 4.0×10^{-8} at $e = 0.995$. In general, for $N \geq 3$,

$$P_N = \frac{4\pi\left[a_2\left(a_2 + 2b_2 - 2b_1\right) - \sum_{j=4}^{N} 2^{j-3}\left(a_{j-1} - b_{j-1}\right)^2\right]}{\frac{1}{2}(a_{N-1}+b_{N-1}) + \sqrt{a_{N-1}b_{N-1}}}, \tag{12}$$

where the denominator equals $a_N + b_N = \frac{1}{2}\left(\sqrt{a_{N-1}} + \sqrt{b_{N-1}}\right)^2$. Combining steps does not save square roots: after N steps the quantities generically lie in a tower of N successive quadratic extensions of $\mathbb{Q}(a,b)$, and we know of no expression for P_N with fewer than N square roots.

In floating point the first term of the numerator suffers from cancellation, because b_2 and b_1 are close unless $b \ll a$. Since $a_1 - b_1 = c_1^2/(2a_2)$ with $c_1 = (a-b)/2$, and $b_2 - b_1 = b_1(a_1-b_1)/(b_2+b_1)$, it can be rewritten exactly as

$$a_2\left(a_2 + 2b_2 - 2b_1\right) = a_2^2 + \frac{b_1 c_1^2}{b_2 + b_1}, \tag{13}$$

in which all terms are positive. The remaining terms $2^{j-3}(a_{j-1}-b_{j-1})^2$ are small for the shapes on which the main formulas use (14) ($b \geq t_s a$), so their cancellation is harmless there. For very flat ellipses these terms become comparable to the first two, and cancellation again amplifies rounding errors (Section 13.1).

4.2. **Truncation and flat ellipses.** With the quantities of Section 3 and (13), the truncated AGM (12) becomes

$$P_N = \frac{4\pi}{a_N + b_N}\left[a_2^2 + \frac{b_1 c_1^2}{b_2 + b_1} - \sum_{j=4}^{N} 2^{j-3}(a_{j-1} - b_{j-1})^2\right]. \tag{14}$$

This is the first branch of each of (9)–(11). For moderate eccentricities its error is tiny and falls very fast as N grows. For $N = 6$, for example, it is below 10^{-50} for $e \leq 0.995$, 2.5×10^{-31} at $b/a = 10^{-3}$ and 1.5×10^{-16} at $b/a = 10^{-6}$. Every truncated AGM fails as $b \to 0$, however:

it tends to $2\pi a$ instead of $4a$, a relative error of 57%, because for $b = 0$ the sum $\sum_{j\le N} 2^{j-1}c_j^2$ equals $a^2(1 - 2^{-N-1})$, while $a_N + b_N = 2^{-N}a$. For flat ellipses, P_N is therefore replaced by a truncated expansion in $t = b/a$.

4.3. **A correction for flat ellipses from Legendre's relation.** Legendre's relation $EK' + E'K - KK' = \pi/2$ [11, §19.7], with $K' = K(k')$, $E' = E(k')$ and $k' = t = b/a$, can be solved for E:

$$E(k) = K(k)\,\mathcal{P}(t) + \mathcal{Q}(t), \qquad \mathcal{P}(t) = 1 - \frac{E(t)}{K(t)}, \qquad \mathcal{Q}(t) = \frac{\pi}{2K(t)}. \tag{15}$$

This identity is exact. For $|t| < 1$, the integrals $K(t)$ and $E(t)$ are $\pi/2$ times power series in t^2 with rational coefficients, so $\mathcal{P}$ and $\mathcal{Q}$ are power series in t^2 with rational coefficients, in fact dyadic rationals, because those of $2K(t)/\pi$ are and $E(t)/K(t) = 1 - t^2 + t(1-t^2)\,(dK/dt)/K(t)$; their first terms are given in (8), and $\mathcal{P}_n$, $\mathcal{Q}_n$ denote the truncations after t^{2n}. The large quantity $K = K(k)$, which grows like $\ln(4a/b)$, must still be estimated, and the AGM provides it through $K = \pi a/(2M(a,b))$. The simplest estimate is $K \approx \pi a/(a_N + b_N)$. A better one follows from expanding one more AGM step without its square root, $M = \frac{1}{2}(a_N + b_N) - (a_N - b_N)^2/\big(8(a_N + b_N)\big) + O\big((a_N - b_N)^4/a_N^3\big)$:

$$K \approx \frac{4\pi a\,(a_N + b_N)}{3a_N^2 + 10a_N b_N + 3b_N^2}. \tag{16}$$

Errors in the estimate of K are multiplied by $\mathcal{P}_n(t) \approx t^2/2$. As $b \to 0$, where the truncated AGM itself is useless, the estimate is poor, with an error of order $\ln(4a/b)$, but its contribution is only of order $t^2 \ln(4a/b)$ and tends to zero. At $b = 0$ the corrected formula gives exactly $4a$, with no special case. Truncated after t^4 ($n = 2$), (15) becomes

$$E \approx 1 + \frac{t^2}{2}\Big(K - \frac{1}{2}\Big) + \frac{t^4}{16}\Big(K - \frac{5}{4}\Big), \tag{17}$$

which is the asymptotic expansion of E for $k' \to 0$ [11, §19.12] with the logarithm eliminated in favour of K; with the simple estimate of K, it is the flat branch of A_3 without the continuity term. Even the first term alone is useful. With $E \approx 1 + \frac{t^2}{2}(K - \frac{1}{2})$, the simple estimate of K, six steps and a switch at $b/a = 10^{-5}$, the maximum error is 1.0×10^{-19}. With the plain fallback $P \approx 4a$, the best switch is $b/a \approx 7.7 \times 10^{-8}$, with error 5.1×10^{-14}.

4.4. **Continuity at the switch.** A formula of this type uses P_N for $b \ge t_s a$ and $4a\big[K\mathcal{P}_n(t) + \mathcal{Q}_n(t)\big]$ for $b < t_s a$. In all cases considered here the truncated AGM overestimates the perimeter, while the corrected expression underestimates it: the omitted terms of the series in (15) sum to a positive quantity, and the estimates of K are slightly too small. The two branches therefore never agree, and every choice of t_s leaves a jump equal to the sum of the two error magnitudes. Since P/a depends only on t, the jump at a fixed t_s is a fixed number, and it can be removed by one further term,

$$P \approx 4a\Big[K\,\mathcal{P}_n(t) + \mathcal{Q}_n(t) + \gamma\,t^{2n+2}\Big], \qquad \gamma = \frac{E_{\mathrm{AGM}}(t_s) - E_{\mathrm{corr}}(t_s)}{t_s^{2n+2}}, \tag{18}$$

where E_{AGM} and E_{corr} are the values of $P/(4a)$ given by the two branches at $t = t_s$. With this γ the formula is exactly continuous, and for the formulas of Section 3 its worst error does not increase: just below the switch, the error now equals that of the AGM branch. Further below the switch the error changes sign once (Section 5). The slope $\partial P/\partial b$ is positive on both sides of the switch. Its relative jump is 1.8×10^{-5} for A_3 and less than 10^{-13} for A_4 and A_6.

For each target format, the number of steps N, the truncation order n, the estimate of K and the switch point t_s were chosen to keep the maximum error below the unit roundoff at low cost, and γ was then computed from (18). The error at every $t < t_s$ is linear in γ, and so is the jump at t_s. Each sample point therefore gives a linear constraint on γ, and the sufficient values defined in Section 3 form an interval, which we computed from the errors of the two branches on a fine sample of shapes (Section 14). The resulting intervals are listed in Table 1.

Such a continuous formula exists for every target accuracy, whatever switch point is chosen.

Proposition 4.1. *Let $0 < t_s \le 1$, $N \ge 3$ and $n \ge 1$. Let $A_{N,n}$ be the formula that equals P_N of (14) for $b \ge t_s a$ and (18) for $b < t_s a$, where K is estimated by $\pi a/(a_N + b_N)$ or by (16) and γ is the continuity coefficient of (18), and let $P^{\mathrm{L}}_{N,n} = 4a\big[K\mathcal{P}_n(t) + \mathcal{Q}_n(t)\big]$, with the same estimate of K, be the Legendre branch without the continuity term. Then:*

(a) *$A_{N,n}$ is continuous for $0 \le b \le a$, equals $4a$ at $b = 0$ and $2\pi a$ at $b = a$;*
(b) $\max\limits_{0\le b\le a} |A_{N,n} - P| \le \max\limits_{t_s a\le b\le a} |P_N - P| + 2 \max\limits_{0\le b\le t_s a} \big|P^{\mathrm{L}}_{N,n} - P\big|$;
(c) *for every $\varepsilon > 0$ there are N_0 and n_0 such that $|A_{N,n}/P - 1| \le \varepsilon$ for $0 \le b \le a$, $N \ge N_0$ and $n \ge n_0$.*

The proof is given in Appendix A. By part (b), the error of the continuous formula is at most that of the AGM branch plus twice that of the Legendre branch; for the formulas of Table 1 it does not increase the maximum error at all, because the two branches err in opposite directions. The proposition also covers $t_s = 1$, where the AGM is used only at $b = a$, so that the formula is essentially the Legendre expansion alone. That case rests on the absolute convergence of the series for $\mathcal{P}$ and $\mathcal{Q}$ up to $t = 1$, which follows from a theorem of Kaluza [21]; the same theorem shows that no coefficient of $\mathcal{Q}$ after the first is positive (numerically, they are all negative). It is of no practical use, however. Even with the exact K, a relative error below 10^{-16} needs 21 terms at $b/a = 0.5$, 128 at $b/a = 0.9$ and 1209 at $b/a = 0.99$, and at $b = a$ the error after n terms decreases only slightly faster than $1/n$, roughly like $1/(n \ln n)$, from 1.3×10^{-3} at $n = 10$ to 4.5×10^{-6} at $n = 1000$. Near the circle the expansion in $t = b/a$ converges slowly, much as the Gauss–Kummer series does near $b = 0$, and the AGM, which converges fastest there, is its natural complement. With a switch at $t_s < 1$ the series converge geometrically, like t_s^{2n}, and the AGM doubly exponentially, which is why a few steps and terms suffice.

5. Accuracy, rounding and cost of the main formulas

Figure 1 shows the errors in 90-digit arithmetic. Each formula attains its maximum at the switch point and is much more accurate away from it. Above the switch the error is that of the truncated AGM, which is positive. Just below it, the continuity term keeps the error positive. As b decreases further, however, the negative error of the Legendre branch decays more slowly than the continuity term γt^{2n+2}, because its truncation part contains the factor $K \sim \ln(4a/b)$ and the error of the estimate of K is multiplied only by $\mathcal{P}_n(t) \approx t^2/2$. The error therefore changes sign, and numerically it does so exactly once, at $b/a = 0.0504$, 0.0200 and 1.01×10^{-4} for A_3, A_4 and A_6, and is negative for all smaller $b > 0$ (checked down to $b/a = 10^{-40}$; as $b \to 0$ the error of the estimate of K dominates). The sign changes appear as the sharp downward spikes in Figure 1. Between the switch point and the sign change, the errors of A_4 and A_6 are close to constant multiples of t^{2n+2} and therefore appear as nearly straight lines; the contribution of the estimate of K, which grows as b decreases, becomes significant only very close to the sign change, so that the lines end abruptly in the spikes. A_3 stays below 1.0×10^{-8} outside $0.081 < b/a < 0.127$ and is about 2×10^{-18} at $e = 0.78$. A_4 stays below 2.5×10^{-18} outside $0.084 < b/a < 0.126$ and below 3.1×10^{-19} for $b/a \le 0.01$. A_6 stays below 4.4×10^{-37} outside $0.0031 < b/a < 0.0035$ and below 9×10^{-41} for $b/a \le 0.0016$. For comparison, R_{II} and I_3 have maximum errors 4.0×10^{-4} and 2.2×10^{-6}, attained for flat ellipses. The six-step AGM P_6 on its own, which A_6 uses for $b \ge 0.0033a$, has an error larger than the binary64 unit roundoff for $b/a \lesssim 1.2 \times 10^{-6}$, and larger than that of I_3 for $b/a \lesssim 5 \times 10^{-16}$; the correction of Section 4.3 is what makes the formulas accurate for flat ellipses. At the closed-form points of Table 2, which all lie on the AGM side of the switches, the errors are listed in Table 3.

In the target arithmetic, rounding dominates. With exactly emulated binary32, A_3 has a maximum error of 2.7×10^{-7} on a sample of about 5000 shapes (Table 5), and 3.6×10^{-7}, about $6u$, on a denser sample of 25 000 shapes. On the same dense sample the minimax formula C_3 evaluated in powers of $\sigma = 1 - h$ (Section 6.5) reaches 2.1×10^{-7}. In binary64, A_4 reaches 5.6×10^{-16} on a similar sample of about 5000 shapes, and 7.1×10^{-16} (about $6u$) on the dense sample. For A_6 we emulated correctly rounded 34-digit decimal arithmetic, whose unit roundoff (5×10^{-34}) is about five times that of binary128. On 1200 shapes with $10^{-12} \le b/a \le 1$

and on $b = 0$, the maximum error was 1.5×10^{-33}, about 3 units, which suggests an error of about 3×10^{-34} in binary128. In all three cases the largest rounding errors occur for moderate eccentricities ($b \geq 0.1a$), in the common first steps. In every format, $b = 0$ gives exactly $4a$ and $b = a$ gives $2\pi a$ to within rounding.

A_3 needs three square roots and two divisions on either branch, together with about 15 multiplications or multiply–adds. A_4 needs four square roots and two divisions per branch, and 15 multiply–adds for $b \geq 0.1a$ or about 40 for $b < 0.1a$. A_6 needs six square roots, two divisions per branch and up to about 45 multiply–adds. The critical path is the chain of dependent multiplications and square roots, $20N$ cycles in the double-precision model of Section 13.1 ($16N$ in binary32). The series and the numerator are evaluated in parallel with it; the estimate of K needs a_N and b_N and adds a division and a few multiply–adds at the end of the flat branch. The latency is thus about 81, 101 and 141 cycles in double precision (67, 83 and 115 in binary32), with a few more cycles on the flat branch.

In our latency model, these costs compare favourably with all alternatives of comparable or better accuracy considered in this note that, like the main formulas, use only arithmetic operations and square roots (for approximations that use a logarithm, see Section 13.1). A_3 has as many square roots as the triple-nested formula I_3, is faster (81 against 110 cycles), and has a maximum error 54 times smaller. In double precision, A_4 has the lowest worst-case latency of these methods that reach full precision for all eccentricities. It is faster than the quadruple-nested formulas (150 cycles) and than a fixed number of AGM steps covering $b/a \geq 10^{-6}$ (7 steps, 161 cycles). An AGM loop that stops as soon as it reaches the target accuracy is a different matter. The main formulas have about the latency of $N = 3$, 4 and 6 steps, and with step counts in exact arithmetic such a loop needs more steps, and is therefore slower, for b/a below about 0.093, 0.091 and 0.0022 in single, double and quadruple precision. It needs the same number of steps for b/a up to about 0.55, 0.55 and 0.093, and fewer above. The number of steps of the loop grows without bound as $b \to 0$ (in double precision, twelve steps at $b/a = 10^{-300}$), and at $b = 0$ the iteration does not converge to the perimeter, whereas the cost of the main formulas is bounded independently of b. The loop also needs a convergence test in every step, which these counts do not include, and in floating point it loses accuracy for flat ellipses (Section 13.1). In single precision, A_3 (67 cycles) is cheaper than C_3 in powers of σ (98 cycles), at about 1.7 times its error on the dense sample. In quadruple precision, square roots and divisions are usually done in software and dominate the cost, so A_6 costs roughly six square roots and two divisions.

6. Nested-radical approximations

We now turn to closed formulas of a different kind, which keep the structure of Ramanujan's second approximation: a single expression with a few nested square roots and no branches. None of them reaches double precision, although C_3, B_4 and C_4 are accurate to single precision in exact arithmetic; they are short, and they shed light on Ramanujan's formula.

6.1. **The form.** We consider approximations

$$P \approx \pi(a+b)\left(1 + \frac{3h}{q + \sqrt{r_1 + \sqrt{r_2 + \cdots + \sqrt{r_{m-1} + \sqrt{Q(h)}}}}}\right), \tag{19}$$

with m square roots (the *depth*) and a polynomial Q of degree at most $d = 2^{m-1}$. The depth-one case $q + \sqrt{Q_0 + Q_1 h}$ contains R_{II}; we call the cases $m = 2, 3, 4$ double, triple and quadruple nested. For integer coefficients it is convenient to allow a numerator $p\,h$ instead of $3h$; dividing p, q by $p/3$, the r_j by $(p/3)^{2^j}$ and Q by $(p/3)^{2^m}$ returns the form (19).

To our knowledge, approximations of the form (19) with two or more nested square roots have not been proposed before. Published refinements of R_{II} keep its single square root and correct its radicand [27], combine it with a Padé approximant found by symbolic regression [23], or

multiply it by an exponential correction factor [4]; logarithmic corrections of R_{II} are discussed in [5].

6.2. **Series matching by unnesting.** Write $D(h) = q + V(h)$ with $V = \sqrt{r_1 + \sqrt{\cdots}}$, and define $W_1 = V^2 - r_1$, $W_{j+1} = W_j^2 - r_{j+1}$, so that $Q = W_{m-1}^2$. Requiring $D = 12G + O(h^n)$ fixes V through h^{n-1}, and then each W_j and Q are determined through h^{n-1} as power series. Since Q is a polynomial of degree d, the coefficients of $h^{d+1}, \dots, h^{n-1}$ of the resulting series must vanish. With $c = V(0) = 12 - q$ and $u_j = W_j(0)$ as unknowns (m of them), each of these coefficients is linear in the innermost unknown u_{m-1}, which makes the equations easy to solve. Counting parameters, the form (19) has $m + d + 1$ free constants, and matching D through h^{d+m} uses all of them. Hence, generically, the highest order of agreement with the Gauss–Kummer series is

$$\varepsilon = O(h^{d+m+2}) : \qquad h^6,\ h^9,\ h^{14} \quad \text{for} \quad m = 2, 3, 4.$$

For $m = 1$ the count predicts agreement through h^3; that R_{II} reaches h^4 is the coincidence in (6).

6.3. **Comparison with Ramanujan's approximation near the circle.**

Proposition 6.1. *Suppose $D(h) = 12G(h) + \delta h^4 + O(h^5)$. Then $\varepsilon(h) = -\frac{\delta}{48} h^5 + O(h^6)$. In particular $|\varepsilon(h)| < |\varepsilon_{\mathrm{II}}(h)|$ for all sufficiently small $h > 0$ if $|\delta| < \frac{9}{8192}$, and only if $|\delta| \le \frac{9}{8192}$.*

Proof. $R - \mathcal{F} = 3h\,(12G - D)/(12G \cdot D) = -3\delta h^5/144 + O(h^6)$ and $\mathcal{F} = 1 + O(h)$. For R_{II} one has $D_4 - 12G_4 = -\frac{405}{16384} + \frac{423}{16384} = \frac{9}{8192}$, which gives $\varepsilon_{\mathrm{II}} = -\frac{3}{131072} h^5 + O(h^6)$. □

A formula can be nowhere worse than R_{II} only if it matches the series through h^4 and satisfies the condition of Proposition 6.1. Matching through h^4 leaves $m + d + 1 - 4$ free parameters: one for double nesting, four for triple nesting and nine for quadruple nesting.

6.4. **A one-parameter family containing Ramanujan's formula.** For double nesting the free parameter can be taken to be $c = 12 - q$, and solving the matching conditions gives the family

$$D_c(h) = 12 - c + \sqrt{c^2 - 4c + c\sqrt{16 - 12h + \frac{9}{2c}\,h^2}}\,, \qquad c > 0. \tag{20}$$

Its radicands stay nonnegative for all $0 \le h \le 1$ only when $c \ge 1.2356$; the expansion at $h = 0$ in Proposition 6.2 exists for every $c > 0$.

Proposition 6.2. *For every $c > 0$, $D_c = 12G + \delta(c) h^4 + O(h^5)$ with*

$$\delta(c) = \frac{9}{8192} \cdot \frac{c^2 + 9c - 18}{c^2}, \qquad \textit{so} \qquad \varepsilon_c(h) = -\frac{3}{131072} \cdot \frac{c^2 + 9c - 18}{c^2}\, h^5 + O(h^6).$$

The expansion is a direct computation; we checked it in exact rational arithmetic for several rational values of c. It has several consequences.

- For $c = 2$ the inner radicand is $(4 - \frac{3}{2}h)^2$, and $D_2 = 10 + \sqrt{4 - 3h}$: *Ramanujan's second approximation is the member $c = 2$ of the family.*
- By Proposition 6.1, the members with $\frac{3}{2} < c < 2$ are more accurate than R_{II} near the circle. Numerically, they are more accurate for *all* eccentricities exactly when $c_0 < c < 2$, where $c_0 \approx 1.50900$; for $\frac{3}{2} < c < c_0$ the error exceeds that of R_{II} near $h \approx 0.47$ ($e \approx 0.98$).
- For $c = \frac{3}{2}(\sqrt{17} - 3) \approx 1.68466$ the h^5 term vanishes, and D_c is the maximally matched double-nested form S_2 of Section 9.
- The rational value $c = \frac{8}{5}$ lies in $(c_0, 2)$, and clearing denominators gives the integer formula I_2 of Section 7, which is therefore, numerically, nowhere less accurate than R_{II}.
- Minimising the maximum error over the members of the family gives $c^* = 1.6083816$ and the formula B_2 of Section 8.

6.5. **A well-conditioned form of the innermost polynomial.** In floating-point arithmetic the innermost polynomial should not be evaluated in powers of h. For the deeper formulas $Q(h)$ becomes small near $h = 1$, while its individual terms $Q_k h^k$ remain large; for B_4, for example, $Q(1) \approx 4.6$ whereas the terms are of size 5×10^7, so Horner's rule loses about seven significant digits. A simple remedy is to expand Q in powers of

$$\sigma = 1 - h = \frac{4ab}{(a+b)^2} = \left(\frac{b_1}{a_1}\right)^2, \tag{21}$$

which can be computed from a and b without cancellation; in the notation of Section 3 it is the squared complementary modulus after one AGM step. Writing

$$Q(h) = \sum_{k=0}^{d} g_k \, \sigma^k, \qquad g_k = (-1)^k \sum_{i=k}^{d} \binom{i}{k} Q_i,$$

we find that the coefficients g_k are positive, except for a single negative one in each of C_3, B_4, S_4 and C_4. As a result the condition number

$$\kappa(Q) = \max_{0 \le h \le 1} \frac{\sum_k |Q_k| \, h^k}{|Q(h)|} \qquad \text{respectively} \qquad \max_{0 \le h \le 1} \frac{\sum_k |g_k| \, \sigma^k}{|Q(h)|}$$

drops from up to 6.5×10^8 in the powers of h to at most 1.35 in the powers of σ (Table 5). In this form Ramanujan's second approximation reads $D = 10 + \sqrt{1 + 3\sigma}$, the family (20) becomes

$$D_c = 12 - c + \sqrt{c^2 - 4c + c\sqrt{4 + \tfrac{9}{2c} + \left(12 - \tfrac{9}{c}\right)\sigma + \tfrac{9}{2c}\sigma^2}}\,,$$

and the integer formulas of Section 7 have innermost polynomials with only positive coefficients:

$$\begin{aligned}
I_2 &: \quad 256 - 192h + 45h^2 = 109 + 102\sigma + 45\sigma^2, \\
I_3 &: \quad Q_3 = 26817808 + 431506176\sigma + 1304128512\sigma^2 + 188006400\sigma^3, \\
I_3' &: \quad Q_3' = 1334299320 + 32290381080\sigma + 153302488488\sigma^2 + 34710405768\sigma^3, \\
I_3'' &: \quad Q_3'' = 272701 + 7646316\sigma + 45530190\sigma^2 + 28142892\sigma^3 + 3933405\sigma^4.
\end{aligned}$$

The coefficients g_k of the real-coefficient formulas are listed in Appendix B. The variable h is still needed for the numerator $3h$, so this form costs one extra division and two extra multiplications. Because σ and h are computed in parallel, the latency in our model is unchanged.

The σ-form also reduces the number of significant digits that the constants need. To keep the maximum error within one per cent of its stated value in double precision, the constants of C_3, B_4 and C_4 need 11, 13 and 14 significant digits in powers of h, but only 8, 11 and 11 in powers of σ. In single precision the σ-form is essential (Section 13.2).

7. Integer-coefficient formulas

Searching over rational parameters with small denominators in the families of Section 6 gives the following formulas, the best we found. All have integer coefficients, and all are, as verified numerically, nowhere less accurate than R_{II}.

Double nesting. With $c = \frac{8}{5}$ in (20), the maximum relative error is 3.04×10^{-5}:

$$I_2: \qquad P \approx \pi(a+b)\left(1 + \frac{15h}{52 + \sqrt{-96 + 10\sqrt{256 - 192h + 45h^2}}}\right). \tag{22}$$

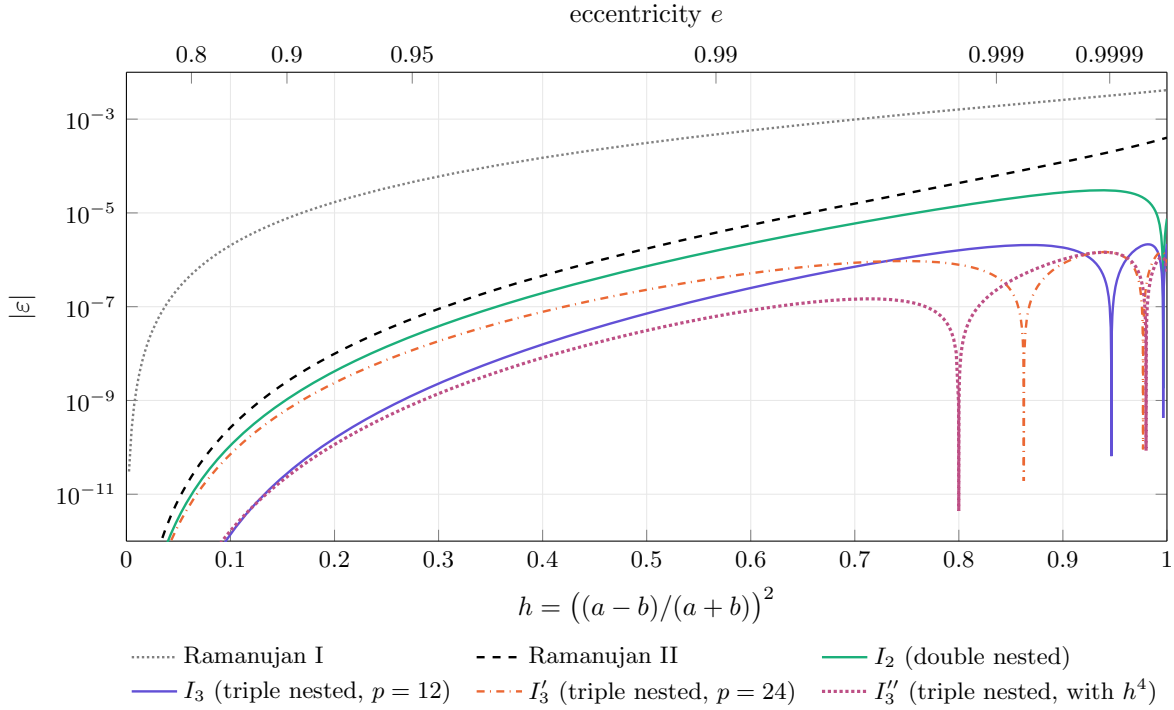

FIGURE 2. Absolute relative error $|\varepsilon|$ of Ramanujan's approximations and of the integer-coefficient nested formulas I_2, I_3, I_3' and I_3'' (I_3'' has an h^4 term in its innermost polynomial), as functions of h (bottom axis) and of the eccentricity (top axis); errors below 10^{-12}, near the circle, lie below the plotted range. The downward spikes are sign changes of the error; the sampling is refined for $h \geq 0.8$ and around them. The spikes of I_2 and I_3 at $h \approx 0.996$ nearly coincide, and a third sign change of I_3, at $h \approx 0.051$, lies below the plotted range.

Triple nesting. The maximum relative errors are 2.17×10^{-6} and 1.48×10^{-6}:

$$I_3: \quad P \approx \pi(a+b)\left(1 + \frac{12h}{40 + \sqrt{-361 + \sqrt{136461 + \sqrt{Q_3(h)}}}}\right), \tag{23}$$

$$Q_3(h) = 1950458896 - 3603782400h + 1868147712h^2 - 188006400h^3,$$

$$I_3': \quad P \approx \pi(a+b)\left(1 + \frac{24h}{81 + \sqrt{-1082 + \sqrt{1237465 + \sqrt{Q_3'(h)}}}}\right), \tag{24}$$

$$Q_3'(h) = 221637574656 - 443026575360h + 257433705792h^2 - 34710405768h^3.$$

Here the innermost polynomial was restricted to degree three. If an h^4 term is allowed, the same search with $p = 12$ gives

$$I_3'': \quad P \approx \pi(a+b)\left(1 + \frac{12h}{41 + \sqrt{-79 + \sqrt{7136 + \sqrt{Q_3''(h)}}}}\right), \tag{25}$$

$$Q_3''(h) = 85525504 - 198868992h + 153559296h^2 - 43876512h^3 + 3933405h^4,$$

which agrees with the series through h^5, is also nowhere less accurate than R_{II}, and has maximum relative error 1.45×10^{-6}. Dropping the h^4 term thus costs little in maximum error (1.48×10^{-6}

for I_3'), but it costs accuracy near the circle: numerically, I_3'' improves on R_{II} by a factor of 55.0 or more at every eccentricity, I_3' only by a factor of 3.32 or more.

7.1. **The relation of I_3 to Ramanujan's second approximation.** Dividing numerator and denominator of (23) by 4 gives

$$I_3: \qquad R(h) = 1 + \frac{3h}{10 + \sqrt{Z(h)}}, \qquad Z(h) = -\frac{361}{16} + \sqrt{\frac{136461}{256} + \sqrt{\frac{Q(h)}{65536}}},$$

with $Q = Q_3$ the cubic in (23). This is R_{II} with its radicand $4 - 3h$ replaced by $Z(h)$; in the notation of Section 6, I_3 has the same value $c = 2$ (equivalently $q = 10$) as R_{II}. Since the formula matches the series at $h = 0$, the nested radicals unwind exactly there:

$$1950458896 = 44164^2, \qquad 136461 + 44164 = 180625 = 425^2, \qquad -361 + 425 = 64,$$

so that $\sqrt{Q(0)/65536} = \frac{44164}{256}$, $\frac{136461}{256} + \frac{44164}{256} = (\frac{425}{16})^2$ and $Z(0) = 4$. Expanding in exact arithmetic,

$$Z(h) = 4 - 3h + 0 \cdot h^2 + 0 \cdot h^3 - \frac{20736}{4692425}\, h^4 + O(h^5), \qquad \frac{20736}{4692425} \approx 0.0044190.$$

Comparing with (6), Z reproduces the two terms of the ideal radicand T that Ramanujan kept, the two vanishing coefficients, and in addition approximates the h^4 term $-\frac{9}{2048} \approx -0.0043945$ of T, which is exactly the term responsible for the h^5 error of R_{II}. Consequently $\delta = -\frac{235503}{38440345600}$ in Proposition 6.1, and

$$\varepsilon_{I_3}(h) = \frac{78501}{615045529600}\, h^5 + O(h^6) \approx 1.28 \times 10^{-7}\, h^5,$$

which is 179 times smaller than the leading error term of R_{II}. In short, I_3 is Ramanujan's second approximation with a corrected radicand: the double-nested radical $Z(h)$ agrees with $4 - 3h$ through h^3 and nearly reproduces the h^4 term of the ideal radicand T. Away from the circle the improvement is smaller, but numerically it is still at least a factor 21.8 at every eccentricity (Table 4).

Figure 2 compares I_2, I_3, I_3' and I_3'' with Ramanujan's two approximations.

8. Real-coefficient formulas that are nowhere worse than Ramanujan's

Dropping the integrality requirement, we minimised the maximum relative error over $0 \le h \le 1$ numerically, subject to the condition $|\varepsilon(h)| \le |\varepsilon_{\mathrm{II}}(h)|$ for all h; for triple and quadruple nesting the results are the best we found rather than certified optima (Section 14). By Proposition 6.1 the condition requires agreement with the series through h^4 and $|\delta| \le 9/8192$. The double-nested optimum B_2 is the member $c^* = 1.6083816$ of the family (20). For B_3 and B_4 there are four (respectively nine) free parameters. They can be taken to be the outer constants q and r_j, the h^4 coefficient δ of Proposition 6.1 and, for B_4, the coefficients $Q_5, \dots, Q_8$; the coefficients $Q_0, \dots, Q_4$ of the innermost polynomial then follow from the matching conditions $D = 12G + \delta h^4 + O(h^5)$. The constants are listed in Appendix B. The maximum errors are

$$B_2: \ 2.30 \times 10^{-5}, \qquad B_3: \ 4.67 \times 10^{-7}, \qquad B_4: \ 8.98 \times 10^{-9},$$

compared with 4.02×10^{-4} for R_{II}, and numerically the improvement over R_{II} is at least a factor 2.62, 46.1 and 9.32, respectively, at every eccentricity (Figure 3). For B_3 and B_4 the smallest improvement occurs in the limit $e \to 0$, where it equals the ratio of the h^5 coefficients. Since the maximum error is attained for flat ellipses, the optimisation constrains the error near the circle only through the condition $|\varepsilon| \le |\varepsilon_{\mathrm{II}}|$; the accuracy of the optimum near the circle is therefore incidental, and B_4 happens to improve on R_{II} there by a smaller factor than B_3. In practice this is immaterial: for $e \le 0.5$ the error of R_{II} itself is below 10^{-16}.

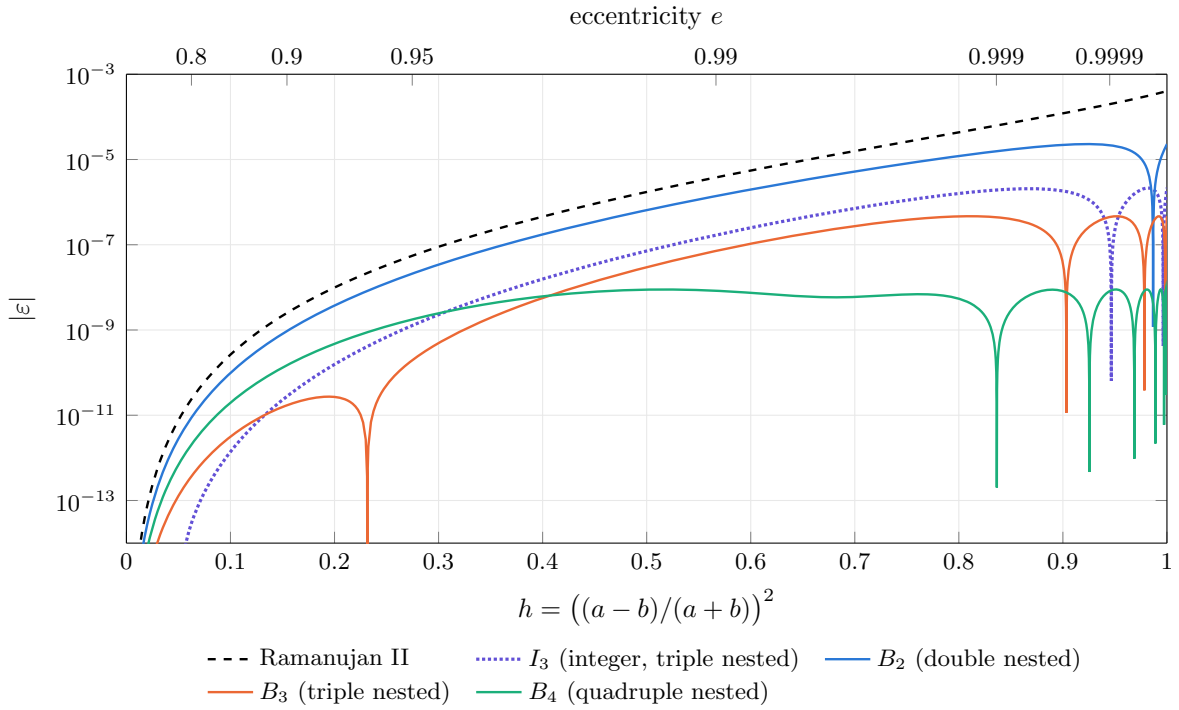

FIGURE 3. Absolute relative error $|\varepsilon|$ of the real-coefficient formulas B_2, B_3, B_4 that are, numerically, nowhere less accurate than R_{II} (dashed), compared with the integer formula I_3 of Section 7 (dotted); errors below 10^{-14}, near the circle, lie below the plotted range. The downward spikes are sign changes of the error; the sampling is refined for $h \geq 0.8$ and around them. The four sign changes with $h > 0.996$ (one of I_3, one of B_3 and two of B_4) merge at the right edge, and that of I_3 at $h \approx 0.051$ lies below the plotted range.

9. Maximal agreement with the Gauss–Kummer series

Using all parameters for series matching, as in Section 6, gives formulas S_2, S_3, S_4 with $\varepsilon = O(h^6)$, $O(h^9)$ and $O(h^{14})$. They play for this form the role that Padé approximants play for rational functions [6]. For triple and quadruple nesting the matching equations have several real solutions; among those we found for which all radicands stay positive on $[0,1]$, we chose the one with the smallest maximum error. S_2 belongs to the family (20) with $c = \frac{3}{2}(\sqrt{17}-3)$:

$$S_2: \qquad P \approx \pi(a+b)\left(1 + \frac{3h}{\frac{33-3\sqrt{17}}{2} + \sqrt{c^2 - 4c + c\sqrt{16 - 12h + \frac{9}{2c}h^2}}}\right), \qquad c = \tfrac{3}{2}\big(\sqrt{17}-3\big).$$

The constants of S_3 and S_4 are given in Appendix B. These formulas are extremely accurate for small and moderate eccentricities: at $e = 0.9$ their relative errors are $+1.5\times10^{-11}$, -6.3×10^{-15} and $+2.5\times10^{-22}$. The last value requires the constants of S_4 to more than the 16 digits of Appendix B; with those, rounding of the constants limits the error at $e = 0.9$ to about 10^{-18} (Section 14). However, their maximum errors, attained at $e = 1$, are comparatively large: 1.42×10^{-4}, 6.14×10^{-5} and 7.83×10^{-6} (Figure 4). Numerically, all three are nevertheless nowhere less accurate than R_{II}, by at least the factors 2.83, 6.55 and 51.4, which are attained at $e = 1$.

10. Minimax formulas

Finally we dropped all constraints and minimised the maximum relative error over $0 \leq h \leq 1$ numerically (for the theory of minimax approximation see, e.g., [24]), within the form (19).

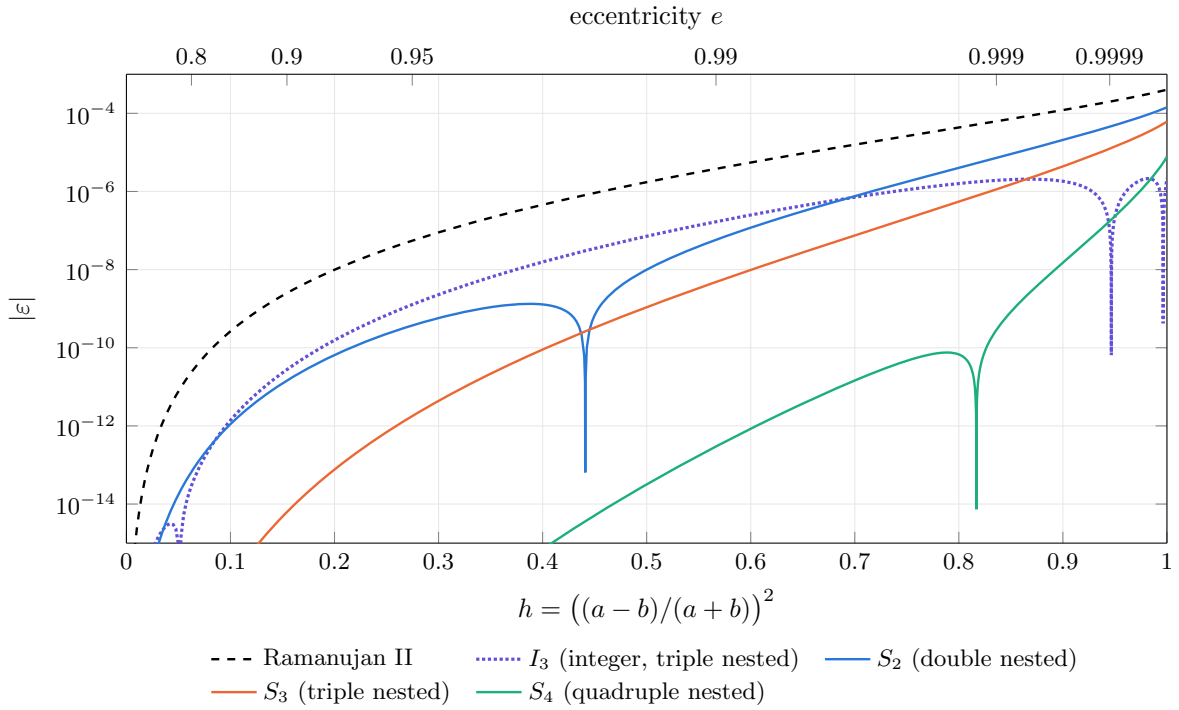

FIGURE 4. Absolute relative error $|\varepsilon|$ of the formulas S_2, S_3, S_4 that agree with the Gauss–Kummer series through h^5, h^8 and h^{13}, compared with R_{II} (dashed), which agrees through h^4, and with the integer formula I_3 of Section 7 (dotted); errors below 10^{-15}, near the circle, lie below the plotted range. The downward spikes are sign changes of the error; the sampling is refined for $h \geq 0.8$ and around them. The error of S_3 does not change sign.

For triple and quadruple nesting the results are the best we found rather than certified optima (Section 14). Their errors nearly equioscillate (Figure 5); the extrema differ by less than 1% for C_2 and C_3 and by up to 2.4% for C_4, whose error also has a smaller lobe next to the circle, for $h < 0.035$. The maximum errors are

$$C_2 : \ 8.03 \times 10^{-7}, \qquad C_3 : \ 4.67 \times 10^{-8}, \qquad C_4 : \ 3.90 \times 10^{-9}.$$

These formulas spend their accuracy uniformly. They do not agree with the Gauss–Kummer series beyond the constant term, so near the circle their error is proportional to h and they are less accurate than R_{II} for small eccentricities: C_2, C_3 and C_4 are more accurate than R_{II} only for e above about 0.960, 0.928 and 0.906, respectively, apart from isolated points near the zeros of their errors. Of the nested-radical formulas of each depth they have the smallest maximum error; the main formulas of Section 3 are far more accurate still, in particular for flat ellipses.

11. Closed-form values

Closed forms for P exist at the *singular moduli*. For a modulus $0 < k < 1$ let $k' = \sqrt{1-k^2}$ be the complementary modulus and $K'(k) = K(k')$. As k increases from 0 to 1, the ratio $K'(k)/K(k)$ decreases continuously from $+\infty$ to 0. Hence for every $N > 0$ there is exactly one modulus k_N with

$$\frac{K'(k_N)}{K(k_N)} = \sqrt{N},$$

for a positive integer N it is called the N-th singular modulus (or singular value). Its complement is $k'_N = k_{1/N}$. Equivalently, the nome $q = e^{-\pi K'/K}$ equals $e^{-\pi\sqrt{N}}$, and the period ratio of the corresponding elliptic curve is $\tau = \mathrm{i}\sqrt{N}$. For a positive integer N this curve has complex multiplication, and this arithmetic structure makes k_N an algebraic number; for instance $k_1 = 1/\sqrt{2}$ and $k_2 = \sqrt{2} - 1$. Moreover, the Chowla–Selberg formula expresses $K(k_N)$ through

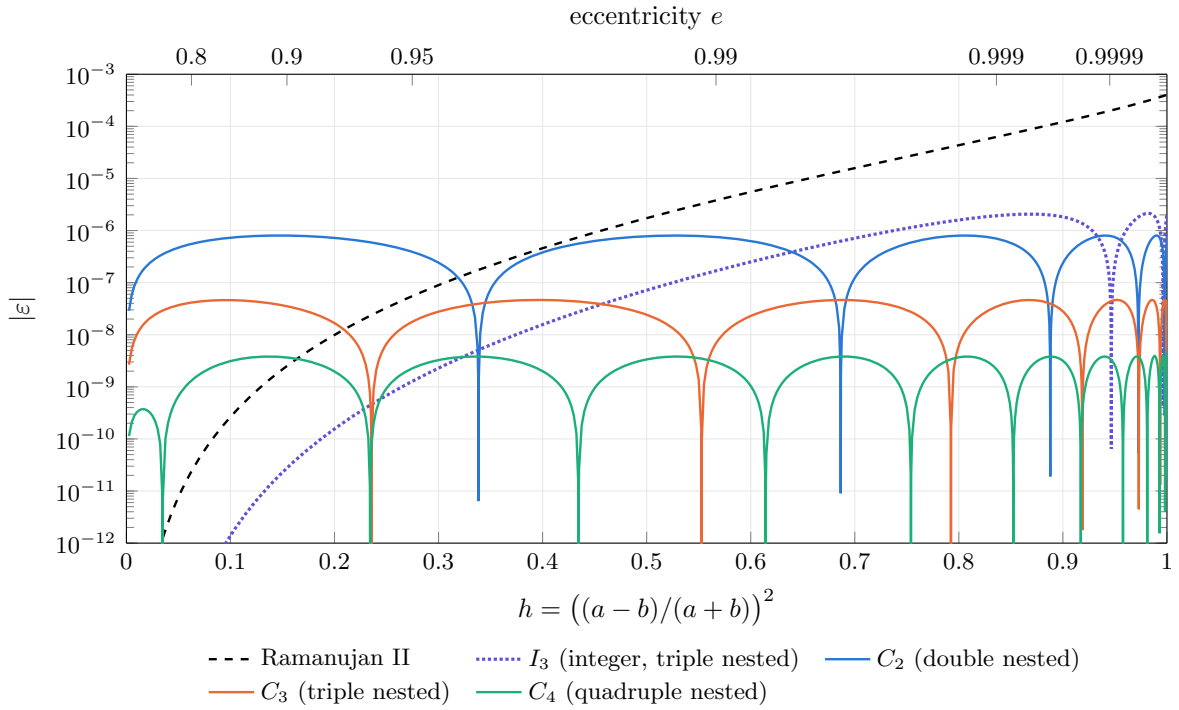

FIGURE 5. Absolute relative error $|\varepsilon|$ of the minimax formulas C_2, C_3, C_4 (for C_3 and C_4 the best found), compared with R_{II} (dashed) and the integer formula I_3 of Section 7 (dotted); errors below 10^{-12}, near the circle, lie below the plotted range. The downward spikes are sign changes of the error; the sampling is refined for $h \geq 0.8$ and around them. The five sign changes with $h > 0.996$ (one each of I_3, C_2 and C_3, and two of C_4) merge at the right edge.

algebraic numbers, powers of π and values of the Gamma function at rational arguments [12], and the elliptic alpha function

$$\alpha(N) = \frac{\pi}{4K(k_N)^2} - \sqrt{N}\Big(\frac{E(k_N)}{K(k_N)} - 1\Big)$$

is again algebraic [8, Ch. 5]. Solving for E gives closed forms for the complete integrals of the second kind at k_N and k'_N:

$$E(k_N) = \Big(1 - \frac{\alpha(N)}{\sqrt{N}}\Big)K_N + \frac{\pi}{4\sqrt{N}\,K_N}, \qquad E(k'_N) = \alpha(N)\,K_N + \frac{\pi}{4K_N}, \qquad K_N = K(k_N),$$

where the second identity follows from the first and Legendre's relation. For $N = 1, 2, 3, 4$,

$$\begin{aligned}
&k_1 = \tfrac{1}{\sqrt{2}}, && \alpha(1) = \tfrac{1}{2}, && K_1 = \frac{\Gamma(\frac14)^2}{4\sqrt{\pi}},\\
&k_2 = \sqrt{2} - 1, && \alpha(2) = \sqrt{2} - 1, && K_2 = \frac{\sqrt{\sqrt{2}+1}\,\Gamma(\frac18)\Gamma(\frac38)}{2^{13/4}\sqrt{\pi}},\\
&k_3 = \tfrac{\sqrt{6}-\sqrt{2}}{4} = \sin 15^\circ, && \alpha(3) = \tfrac{\sqrt{3}-1}{2}, && K_3 = \frac{3^{1/4}\,\Gamma(\frac13)^3}{2^{7/3}\pi},\\
&k_4 = 3 - 2\sqrt{2}, && \alpha(4) = 6 - 4\sqrt{2}, && K_4 = \frac{2+\sqrt{2}}{4}\,K_1.
\end{aligned}$$

Since $P = 4aE(e)$, these four values of N give seven eccentricities in $(0, 1)$ with closed-form perimeters (with $k_1 = k'_1$), listed in Table 2; every further positive integer N gives two more. With the lemniscate constant $\varpi = \Gamma(\frac14)^2/(2\sqrt{2\pi}) = \sqrt{2}\,K_1$, three of them take a particularly

simple form:

$$P\bigl(e=\tfrac{1}{\sqrt2}\bigr)=\sqrt2\,a\Bigl(\varpi+\frac{\pi}{\varpi}\Bigr),$$
$$P\bigl(e=3-2\sqrt2\bigr)=2a\Bigl(\varpi+\frac{(\sqrt2-1)\pi}{\varpi}\Bigr),$$
$$P\bigl(e=2\sqrt{3\sqrt2-4}\bigr)=2(\sqrt2-1)\,a\Bigl(\varpi+\frac{2\pi}{\varpi}\Bigr).$$

We evaluated these expressions in 80-digit arithmetic, with the Gamma function computed from Stirling's series, and checked them against the AGM; the two agree to at least 76 significant digits. Table 3 lists the relative errors of all formulas at these points, computed with 80 significant digits, so that even errors far below double precision are resolved; for B_3, B_4, S_3 and S_4 the matched coefficients were computed to high precision (Section 14).

TABLE 2. The seven eccentricities e with closed-form perimeters for $N=1,\dots,4$, the corresponding axis ratio b/a, the value of h, and $P/a=4E(e)$. Here $K_N=K(k_N)$ and $\varpi=\sqrt2\,K_1$ are as in the text.

	e	b/a	h	P/a	numerical value of P/a
k_1	$1/\sqrt2$	$1/\sqrt2$	0.029437	$2K_1+\dfrac{\pi}{K_1}=\sqrt2\Bigl(\varpi+\dfrac{\pi}{\varpi}\Bigr)$	5.402575524190702010081
k_2	$\sqrt2-1$	$\sqrt{2\sqrt2-2}$	0.002211	$2\sqrt2\,K_2+\dfrac{\pi}{\sqrt2\,K_2}$	6.004324182524975645981
k_2'	$\sqrt{2\sqrt2-2}$	$\sqrt2-1$	0.171573	$4(\sqrt2-1)K_2+\dfrac{\pi}{K_2}$	4.635590099210058269657
k_3	$\frac{\sqrt6-\sqrt2}{4}$	$\frac{\sqrt6+\sqrt2}{4}$	0.000300	$\dfrac{2(3+\sqrt3)}{3}K_3+\dfrac{\pi}{\sqrt3\,K_3}$	6.176601987658693464746
k_3'	$\frac{\sqrt6+\sqrt2}{4}$	$\frac{\sqrt6-\sqrt2}{4}$	0.346674	$2(\sqrt3-1)K_3+\dfrac{\pi}{K_3}$	4.305620452305612100270
k_4	$3-2\sqrt2$	$2\sqrt{3\sqrt2-4}$	0.000056	$2\Bigl(\varpi+\dfrac{(\sqrt2-1)\pi}{\varpi}\Bigr)$	6.236869782889715524 76
k_4'	$2\sqrt{3\sqrt2-4}$	$3-2\sqrt2$	0.500000	$2(\sqrt2-1)\Bigl(\varpi+\dfrac{2\pi}{\varpi}\Bigr)$	4.157327340030711915898

12. Summary of accuracy and cost

Table 4 collects, for every formula, the order of agreement with the Gauss–Kummer series, the maximum relative error over all eccentricities, the smallest improvement factor over R_{II}, and the estimated cost compared with the AGM steps needed to reach at least the same accuracy. The minimum improvement factor is $\min_{0<e\le1}|\varepsilon_{\mathrm{II}}(e)|/|\varepsilon(e)|$, determined numerically. Where it is attained depends on the formula. For A_3, A_4 and A_6 it is attained at the switch points. For I_3', B_3 and B_4 it is the limit $e\to0$ and equals the ratio of the h^5 coefficients (Proposition 6.1). For I_2, B_2 and I_3 it is attained at large eccentricity: at $e\approx0.966$, 0.965 and 0.994, while the ratio tends to 2.46, 2.76 and 179 as $e\to0$. For S_2, S_3 and S_4, which agree with the series beyond h^4, it is attained at $e=1$, and for I_3'', which agrees with it through h^5, at $e\approx0.981$.

Some observations:

- The main formulas A_3, A_4 and A_6 of Section 3 are designed for full precision in a given format: A_3 for single, A_4 for double and A_6 for quadruple precision. In the latency model, A_3 (81 cycles) is faster than the double- and triple-nested formulas (86–114 cycles) and has a smaller maximum error than all of them, and A_4 (101 cycles) is faster than the quadruple-nested formulas (150 cycles) while being accurate to full double precision. Of the closed formulas in this note that use only arithmetic operations and square roots, only R_{I} and R_{II} are cheaper than A_3. The nested formulas keep the advantages of a single expression without branches and of a smaller operation count, which matters when throughput rather than latency limits the speed.

TABLE 3. Relative error ε of each formula at the closed-form points of Table 2, computed with 80 significant digits (for B_3, B_4, S_3 and S_4 with high-precision matched coefficients, see Section 14). Here xek means $x \times 10^k$.

	k_4	k_3	k_2	k_1	k_2'	k_3'	k_4'
e	0.171573	0.258819	0.414214	0.707107	0.910180	0.965926	0.985171
R_{I}	−3.4e−16	−5.3e−14	−2.1e−11	−5.0e−8	−1.1e−5	−9.5e−5	−3.1e−4
R_{II}	−1.2e−26	−5.6e−23	−1.2e−18	−5.3e−13	−4.4e−9	−2.0e−7	−1.7e−6
A_3	+2.7e−42	+1.9e−36	+1.7e−29	+1.8e−20	+4.1e−14	+2.5e−11	+1.1e−9
A_4	$< 10^{-75}$	+6.0e−74	+4.5e−60	+5.4e−42	+3.1e−29	+1.3e−23	+2.8e−20
A_6	below 10^{-75} at all seven points						
I_2	+5.0e−27	+2.3e−23	+4.9e−19	+2.2e−13	+1.9e−9	+8.6e−8	+7.3e−7
I_3	+6.9e−29	+3.1e−25	+6.5e−21	+1.2e−15	−5.6e−11	−6.0e−9	−7.2e−8
I_3'	+3.7e−27	+1.7e−23	+3.6e−19	+1.5e−13	+1.1e−9	+3.8e−8	+2.3e−7
I_3''	+4.6e−32	+1.1e−27	+1.8e−22	+1.0e−15	+4.5e−11	+3.4e−9	+3.1e−8
B_2	+4.5e−27	+2.0e−23	+4.4e−19	+1.9e−13	+1.7e−9	+7.7e−8	+6.5e−7
B_3	−2.7e−28	−1.2e−24	−2.6e−20	−9.9e−15	−2.3e−11	+1.8e−9	+3.0e−8
B_4	−1.3e−27	−6.0e−24	−1.3e−19	−5.1e−14	−2.4e−10	−4.1e−9	−8.9e−9
S_2	+3.4e−32	+8.3e−28	+1.3e−22	+7.4e−16	+2.7e−11	+1.1e−9	−1.0e−8
S_3	−3.9e−46	−1.5e−39	−9.5e−32	−1.4e−21	−1.7e−14	−2.0e−11	−1.1e−9
S_4	+7.2e−71	+1.2e−60	+1.7e−48	+1.1e−32	+1.2e−21	+6.7e−17	+3.2e−14
C_2	+6.5e−10	+3.5e−9	+2.6e−8	+3.0e−7	+7.9e−7	−5.3e−8	−7.8e−7
C_3	+6.0e−11	+3.2e−10	+2.4e−9	+2.6e−8	+2.9e−8	−4.1e−8	−2.4e−8
C_4	−2.8e−12	−1.5e−11	−1.0e−10	−1.7e−10	+3.2e−9	−3.8e−9	+3.4e−9

- In the families B and C, each additional level of nesting lowers the maximum error by a factor of roughly 10 to 50, at a cost of one square root, one addition and a few multiply–adds. The series-matched formulas S_j improve more slowly, because agreement at $h = 0$ does little for flat ellipses.
- The integer formulas lose little against the real-coefficient formulas of the same depth with the same property, nowhere less accurate than R_{II}: I_2 is within a factor 1.3 of B_2, and I_3' and I_3'' within a factor 3.2 of B_3.
- In the latency model (Section 13) the nested formulas cost between 1.4 and 2.4 times as much as R_{II}. To reach the same maximum error in exact arithmetic, the AGM needs 3 or 4 steps (81–101 cycles) for $e \le 0.995$ and 5 or 6 steps (121–141 cycles) for $b/a \ge 10^{-6}$. R_{II} (62 cycles) is therefore clearly cheaper than the AGM at its accuracy. The double-nested formulas (86 cycles) cost slightly more than the three AGM steps that suffice for $e \le 0.995$, but much less than the five steps needed for $b/a \ge 10^{-6}$. The triple-nested formulas (110–114 cycles) are slower than the AGM for $e \le 0.995$ and faster for $b/a \ge 10^{-6}$, and the quadruple-nested formulas (150 cycles) are slower in both cases. Unlike any fixed number of AGM steps, however, the nested formulas cover all eccentricities, including $b = 0$, at a fixed cost without branches; this, and their form as explicit expressions, is their main attraction (vectorised code, hardware implementations).

13. Estimating the computational cost

Comparing the cost of a closed formula with that of an iterative method requires some care, because the answer depends on the hardware, the compiler and the accuracy required. We first discuss double precision, using three complementary estimates, and then single precision, where the comparison changes.

13.1. **Double precision.**

Operation counts. All methods start from a and b. The nested formulas compute $s = a + b$, $\lambda = (a-b)/s$, $h = \lambda^2$, evaluate the innermost polynomial by Horner's rule (d fused multiply–adds,

TABLE 4. Summary. m: number of square roots; deg: degree of the innermost polynomial; n: the formula agrees with the Gauss–Kummer series through h^n, and c_{n+1} is the leading coefficient of $\varepsilon(h) = c_{n+1}h^{n+1} + \dots$ (for the formulas C_j the series agrees only through h^0); $\max|\varepsilon|$: maximum relative error for $0 \le e \le 1$; gain: $\min_{0<e\le1} |\varepsilon_{\mathrm{II}}|/|\varepsilon|$, determined numerically (a dash if the formula is somewhere less accurate than R_{II}); ops: square roots / divisions / multiplications or multiply–adds / additions; lat.: critical-path latency in cycles (Section 13); N: AGM steps needed to reach $\max|\varepsilon|$ for $e \le 0.995$ and for $b/a \ge 10^{-6}$; AGM lat.: latency of the AGM with the larger N. A_3, A_4 and A_6 are the main formulas of Section 3 (operation counts for the more expensive branch), to which the series and AGM columns do not apply. In the last three rows, $\max|\varepsilon|$ is the unit roundoff of binary32, binary64 and binary128, and N is the number of AGM steps needed to reach it in exact arithmetic; in floating-point arithmetic, rounding prevents the AGM from reaching it for flat ellipses (Sections 13.1 and 13.2). All latencies are given in the double-precision model; the binary32 model gives 115 cycles for the single-precision AGM, and in quadruple precision, where square roots are usually computed in software, N is the better measure of cost. Here xek means $x \times 10^k$.

Formula	m	deg	n	c_{n+1}	$\max\|\varepsilon\|$	gain	ops	lat.	N	AGM lat.
R_{I}	1	1	2	−1.95e−3	4.16e−3	–	1/0/5/1	32	2/4	101
R_{II}	1	1	4	−2.29e−5	4.02e−4	–	1/2/5/3	62	3/5	121
A_3	3	–	–	–	4.00e−8	289	3/2/15/7	81	–	–
A_4	4	–	–	–	4.09e−17	2.8e11	4/2/41/9	101	–	–
A_6	6	–	–	–	8.11e−37	4.1e32	6/2/45/11	141	–	–
I_2	2	2	4	+9.30e−6	3.04e−5	2.34	2/2/6/4	86	3/5	121
I_3	3	3	4	+1.28e−7	2.17e−6	21.8	3/2/7/5	110	3/5	121
I_3'	3	3	4	+6.89e−6	1.48e−6	3.32	3/2/7/5	110	3/5	121
I_3''	3	4	5	+1.54e−6	1.45e−6	55.0	3/2/8/5	114	3/5	121
B_2	2	2	4	+8.30e−6	2.30e−5	2.62	2/2/6/4	86	3/5	121
B_3	3	4	4	−4.96e−7	4.67e−7	46.1	3/2/8/5	114	3/5	121
B_4	4	8	4	−2.46e−6	8.98e−9	9.32	4/2/12/6	150	4/6	141
S_2	2	2	5	+1.13e−6	1.42e−4	2.83	2/2/6/4	86	3/5	121
S_3	3	4	8	−7.48e−8	6.14e−5	6.55	3/2/8/5	114	3/5	121
S_4	4	8	13	+2.56e−11	7.83e−6	51.4	4/2/12/6	150	3/5	121
C_2	2	2	0	+1.17e−5	8.03e−7	–	2/2/6/4	86	3/5	121
C_3	3	4	0	+1.08e−6	4.67e−8	–	3/2/8/5	114	3/6	141
C_4	4	8	0	−5.02e−8	3.90e−9	–	4/2/12/6	150	4/6	141
AGM, single prec.					6.0e−8				3/6	141
AGM, double prec.					1.1e−16				4/7	161
AGM, quadruple prec.					9.6e−35				5/8	181

where d is its degree), take m square roots with one addition each, and finish with one division and one fused multiply–add for $\pi s\,(1 + 3h/D)$. R_{I} is evaluated as $\pi(3s - \sqrt{(3a+b)(a+3b)})$ without division. In the well-conditioned form of Section 6.5 the polynomial is evaluated in $\sigma = 4ab/s^2$, which adds one division and two multiplications. The AGM (7) costs, per step, one square root, two additions and three multiplications, plus a division at the end. Table 4 lists the counts as (square roots, divisions, multiplications or multiply–adds, additions).

Latency model. A single evaluation of any of these formulas is a chain of dependent operations, so on a modern out-of-order processor its time is governed by the length of the critical path, not by the number of operations. We take latencies of 4 cycles for addition, multiplication and fused multiply–add, 13 cycles for division and 16 cycles for square root in double precision, which is representative of current x86-64 cores [14]. Along the critical path, the prologue ($a \pm b$, division, squaring) takes 21 cycles, Horner's rule $4d$, each nesting level 20 (square root plus addition),

and the epilogue (division and multiply–add) 17, so

$$L_{\text{nested}}(m,d) = 38 + 4d + 20m \text{ cycles}, \qquad L_{R_{\text{I}}} = 32, \qquad L_{\text{AGM}}(N) = 20N + 21.$$

The AGM step is limited by the dependent multiplication and square root $b_{j+1} = \sqrt{a_j b_j}$ (20 cycles); the other operations of a step run in parallel. Thus R_{II} costs 62 cycles, double nesting 86, triple nesting 110 to 114, quadruple nesting 150, and the AGM 81, 101, 121, 141 and 161 cycles for $N = 3, \dots, 7$. In throughput-bound settings, such as many independent evaluations in vector registers, the counts of square roots and divisions matter more than the latency; the nested formulas use m square roots and two divisions (three in the σ-form), the AGM uses N square roots and one division.

Number of AGM steps. To compare at equal accuracy, we determined for each formula the smallest N such that the truncated AGM (7), with M replaced by $(a_N + b_N)/2$, has a relative error not larger than the maximum error of the formula. The error of the truncated AGM grows as $b/a \to 0$ (roughly one extra step is needed whenever $\log(4a/b)$ doubles), so N depends on the range of shapes considered. We report N for $e \le 0.995$ (that is, $b/a \ge 0.1$) and for $b/a \ge 10^{-6}$, evaluating the truncated AGM in 60-digit arithmetic at $b/a \in \{1, 0.5, 0.2, 0.1, \dots, 10^{-6}\}$. Full double precision ($2^{-53} \approx 1.1 \times 10^{-16}$) needs $N = 4$ and $N = 7$ steps, respectively; the unit roundoffs of single and quadruple precision (2^{-24} and 2^{-113}) need $N = 3$ and 6, and $N = 5$ and 8 steps (in exact arithmetic). No fixed N suffices for all shapes: double precision needs 12 steps at $b/a = 10^{-300}$, and at $b = 0$ every truncated AGM gives $2\pi a$. An AGM loop with a stopping test therefore needs a special case for $b = 0$: there $b_j = 0$ and $c_j = a_j$ for all $j \ge 1$, so a relative test on c_j/a_j never succeeds.

Rounding in the AGM. The step counts above assume exact arithmetic. In floating point, the sum form (7) computes $a^2 - \sum_j 2^{j-1} c_j^2 = a^2 E/K$ as a difference of nearly equal numbers, so rounding errors are amplified by a factor of order K/E. This factor grows like $\ln(4a/b)$, from about 15 at $b/a = 10^{-6}$ to about 700 at $b/a = 10^{-300}$; Section 13.2 discusses the consequences in single precision. In binary64, the AGM (7) iterated to convergence has a maximum relative error of 4.0×10^{-15} for $10^{-6} \le b/a \le 1$ and 1.4×10^{-13} for $10^{-300} \le b/a \le 10^{-6}$ (on 401 logarithmically spaced points in each range). With the cancellation-free numerator of (14) these errors drop to 4.4×10^{-16} and 3.8×10^{-15}, while A_4 has 4.4×10^{-16} and 2.2×10^{-16} on the same points. Thus in double precision even a converged AGM does not quite reach full accuracy for flat ellipses, whereas A_4 does.

Library approximations. Approximations $E \approx p_1(\eta) + p_2(\eta) \ln(1/\eta)$ with polynomials p_1, p_2 in $\eta = (b/a)^2$ go back to Hastings [18] (see [1, 17.3.36]; degree 4, maximum relative error 1.6×10^{-8}), and Cody [13] gave minimax coefficients up to degree 10 (maximum error 3.8×10^{-18}). With a library logarithm of 20 to 50 cycles, the degree-10 approximation takes about 65 to 79 cycles in our model, less than A_4. Its accuracy is fixed by the published coefficients, however: Cody's table ends at degree 10, so quadruple precision would require a new fit. Fukushima's methods [15, 16, 17] split the range of the parameter $m = e^2$ into intervals with separate polynomials or rational functions and use the logarithmic form near $m = 1$; the method of [16], for example, uses Taylor polynomials of degree up to 20 on ten intervals of $0 < m \le 0.9$ and stores 362 coefficients in double precision, and its author notes that all of them must be recomputed for each precision. The main formulas need neither a logarithm nor piecewise coefficient tables, are continuous by construction, and extend to any precision by Proposition 4.1, A_6 covering binary128.

Measured time. As a sanity check we timed straightforward implementations in CPython (2000 shapes, best of five runs). Interpreter overhead dominates these timings, so they mainly count operations: R_{II} took 149 ns, the double-, triple- and quadruple-nested forms 188, 232 and 326 ns, and the AGM 493 ns with $N = 5$ and 607 ns with $N = 7$. A compiled implementation would follow the latency model more closely.

Asymptotic complexity. At arbitrary precision p (in bits) and for a fixed shape, the AGM needs $O(\log p)$ steps, each a multiplication and a square root at precision p, for a total of $O(M(p) \log p)$ bit operations, where $M(p)$ is the cost of multiplication [9, 26, 8]. Uniformly in the shape, the number of steps is $O\big(\log p + \log\log(4a/b)\big)$ for $0 < b \le a$, so the second term matters only for

extremely flat ellipses. The nested-radical formulas have fixed accuracy and cannot be refined; their cost is $O(1)$ floating-point operations, and they are useful only up to their stated accuracy. The construction of the main formulas extends to any accuracy (Proposition 4.1), but the number of series terms then grows linearly with the number of digits, so at high precision the AGM itself is preferable. Carlson's duplication algorithm for symmetric elliptic integrals [10, 11] converges only linearly (by a fixed factor per step), so for complete integrals at high precision the AGM is preferable; in double precision both need a handful of square roots.

13.2. **Single precision.** In single precision (IEEE binary32 [19], unit roundoff $u = 2^{-24} \approx 6.0 \times 10^{-8}$) the comparison changes. We emulated binary32 arithmetic exactly: every addition, multiplication, division and square root was correctly rounded to 24 bits, all constants were stored in binary32, and Horner's rule used fused multiply–adds. With this arithmetic we evaluated the nested formulas and the AGM for 4997 axis ratios $b/a \in [10^{-6}, 1]$, and the main formulas on about 5000 shapes with b/a down to 10^{-40} and $b = 0$, with separately rounded multiplications and additions. Table 5 shows the results; three effects stand out.

The accuracy floor. Rounding limits every method to a few units of u. The well-conditioned formulas reach about 1.6×10^{-7}, which is less than $3u$. Formulas whose design error lies below this level gain nothing from it: C_3, B_4 and C_4 everywhere, and S_3, S_4 and I_3'' for moderate eccentricities. Quadruple nesting is therefore pointless in single precision.

Conditioning of the inner polynomial. Evaluated in powers of h, the deeper formulas lose much more accuracy. C_3 degrades to 1.1×10^{-6} and B_4 to 1.4×10^{-4}, and for C_4 rounding even makes the innermost radicand negative for 133 of the 4997 shapes. In powers of σ (Section 6.5) every formula is accurate to within rounding.

The AGM loses accuracy for flat ellipses. The truncated AGM (7) computes $a^2 - \sum_j 2^{j-1} c_j^2 = a^2 E/K$ as a difference of nearly equal numbers. Since K grows like $\log(4a/b)$ for flat ellipses, rounding errors are amplified by a factor of order K/E. In binary32 the AGM therefore stalls at 4.4×10^{-7} for $e \le 0.995$, reached after $N = 3$ steps, and at 2.0×10^{-6} for $b/a \ge 10^{-6}$, reached after $N = 5$ steps; more steps do not help. A modified AGM that avoids this subtraction [2] did not do better in our tests: about 9×10^{-7} at its best number of steps, and worse with more steps. Both losses can largely be avoided: the main formulas of Section 3 remove the cancellation by the exact rewriting (13) of the first terms and replace the AGM for flat ellipses by the Legendre-relation correction of Section 4.3.

Cost. With binary32 latencies of about 11 cycles for division and 12 for square root (and 4 for addition, multiplication and multiply–add [14]), the latency model becomes

$$L_{\mathrm{nested}}(m, d) = 34 + 4d + 16m, \qquad L_{R_{\mathrm{I}}} = 28, \qquad L_{\mathrm{AGM}}(N) = 16N + 19,$$

that is, 54 cycles for R_{II}, 74 for double nesting, 94–98 for triple nesting and 130 for quadruple nesting, against 67, 83 and 99 cycles for the AGM with $N = 3, 4, 5$. The consequences are as follows.

- For $b/a \ge 10^{-6}$ the binary32 AGM reaches its best accuracy, only 2.0×10^{-6}, with $N = 5$ steps (99 cycles). The triple-nested formula C_3 in σ-form reaches 2.0×10^{-7} for all these shapes in 98 cycles. In single precision C_3 is thus as fast as the AGM and about ten times more accurate.
- For $e \le 0.995$ the plain AGM with $N = 3$ (67 cycles) reaches 4.4×10^{-7}; the corrected three-step formula A_3 of Section 3 reaches 2.7×10^{-7} for all shapes at about the same cost.
- As in double precision, R_{II} (54 cycles) is cheaper than the AGM at its accuracy, and the double-nested formulas (74 cycles) are slightly slower than three AGM steps (67 cycles) for $e \le 0.995$ but faster than the five steps needed for $b/a \ge 10^{-6}$.
- The main formulas of Section 3 avoid most of the AGM's loss once the numerator is written in the cancellation-free form (13). The three-step formula A_3 then reaches 2.7×10^{-7} for all shapes, including $b = 0$, in 67 cycles. This is the cheapest way we found to obtain nearly full single precision for every eccentricity without a logarithm; C_3 in σ-form is somewhat more accurate (2.0×10^{-7}) but costs 98 cycles. The four-

and six-step formulas A_4 and A_6 gain nothing over A_3 in binary32, because rounding dominates.

In vectorised code and on graphics processors, where single precision is the common choice, the fixed operation count of the formulas is an additional advantage; the nested formulas are moreover free of branches, while the main formulas need a select between their two branches. Note, however, that "fast-math" square roots and divisions on such hardware are often not correctly rounded, which raises all of the above floors somewhat.

TABLE 5. Single precision (binary32). κ_h, κ_σ: condition numbers of the innermost polynomial in powers of h and of $\sigma = 1-h$ (Section 6.5); $\max|\varepsilon|$: maximum relative error with exactly emulated binary32 arithmetic over 4997 axis ratios $b/a \in [10^{-6}, 1]$ (for A_3, A_4 and A_6 over about 5000 shapes with b/a down to 10^{-40} and $b = 0$, see Section 13.2), with the polynomial evaluated in powers of h or of σ, and in the last error column over $e \le 0.995$ only (in powers of σ); NaN: rounding made a radicand negative (for 133 shapes); lat.: binary32 critical-path latency in cycles. For comparison, the design errors (exact arithmetic) are listed in Table 4. Here xek means $x \times 10^k$.

			$\max\|\varepsilon\|$ in binary32			
Formula	κ_h	κ_σ	powers of h	powers of σ	σ, $e \le 0.995$	lat.
R_{I}	–	–	4.2e−3	4.2e−3	8.4e−4	28
R_{II}	7.0	1.00	4.0e−4	4.0e−4	1.2e−5	54
I_2	4.5	1.00	3.0e−5	3.0e−5	4.5e−6	74
I_3	2.8e2	1.00	2.3e−6	2.3e−6	5.8e−7	94
I_3'	7.2e2	1.00	1.6e−6	1.6e−6	8.6e−7	94
I_3''	1.8e3	1.00	1.5e−6	1.5e−6	2.7e−7	98
B_2	4.5	1.00	2.3e−5	2.3e−5	4.0e−6	74
B_3	2.8e3	1.00	6.0e−7	5.9e−7	2.9e−7	98
B_4	3.6e7	1.07	1.4e−4	1.8e−7	1.6e−7	130
S_2	4.6	1.00	1.4e−4	1.4e−4	5.0e−7	74
S_3	1.1e2	1.00	6.1e−5	6.1e−5	1.6e−7	98
S_4	2.2e4	1.00	7.8e−6	7.9e−6	1.6e−7	130
C_2	3.7e2	1.00	9.4e−7	9.4e−7	9.4e−7	74
C_3	7.3e4	1.01	1.1e−6	2.0e−7	1.8e−7	98
C_4	6.5e8	1.35	NaN	1.6e−7	1.6e−7	130
AGM, $N = 3$				9.2e−2	4.4e−7	67
AGM, $N = 4$				1.2e−3	4.4e−7	83
AGM, $N = 5$				2.0e−6	4.4e−7	99
A_3 (Section 3)				2.7e−7	2.7e−7	67
A_4 (Section 3)				2.7e−7	2.7e−7	83
A_6 (Section 3)				2.7e−7	2.7e−7	115

14. Numerical methods and verification

The reference values of $\mathcal{F}(h)$ were computed with the AGM (7), written in terms of $\lambda = \sqrt{h}$ to avoid cancellation ($b/a = (1-\lambda)/(1+\lambda)$ and $e = 2\sqrt{\lambda}/(1+\lambda)$), in double precision on grids of 21 600 points and in 80-digit decimal arithmetic for all reported values (90 digits for Figure 1 and for the refined sampling of Figures 2–5). Power series were composed in exact rational arithmetic for the integer formulas and in 80-digit arithmetic otherwise.

Each main formula was evaluated in 80-digit arithmetic at about 3700 axis ratios: $b/a = 10^{-j/400}$ for $0 \le j \le 3200$, $b/a = 10^{-j/10}$ for $81 \le j \le 400$, 199 points just below its switch point, and $b = 0$. The reference values were computed with the AGM (7) run to convergence. The coefficients of $\mathcal{P}$ and $\mathcal{Q}$ were computed in exact rational arithmetic from the series of K and E. The continuity coefficients were computed from (18) in 80-digit arithmetic, and the intervals

of sufficient γ from the linear dependence of the error on γ at the same points. Rounding errors were measured with exactly emulated binary32 and binary64 arithmetic and with correctly rounded 34-digit decimal arithmetic (Section 5). Figure 1 and the sign changes of the errors reported in Section 5 were computed in 90-digit arithmetic, down to $b/a = 10^{-40}$. The term counts quoted after Proposition 4.1 were computed with K and E from the AGM and with the coefficients of $\mathcal{P}$ and $\mathcal{Q}$ to 50 digits.

The maximally matched formulas were obtained by solving the matching equations of Section 6 with Newton's method in 80-digit arithmetic, starting from many initial points, which gave residuals below 10^{-70}. The minimax and constrained formulas were obtained by variable projection: for fixed outer constants $(q, r_1, \ldots, r_{m-1})$ the error is, to first order, linear in the coefficients of the innermost polynomial, which were fitted by Lawson's iteratively reweighted least-squares algorithm for discrete minimax approximation, while the outer constants were optimised with the Nelder–Mead method from many random starting points. The resulting maxima were then refined by golden-section search in 80-digit arithmetic. The optimisation landscapes, especially for $m = 4$, have many local minima, so the real-coefficient optima (B_3, B_4, C_3, C_4) are the best found rather than certified global optima.

The property "nowhere less accurate than R_{II}" was checked in three ways: near the circle by Proposition 6.1, with the h^5 coefficient computed exactly or in high precision; on the double-precision grid wherever $|\varepsilon_{\mathrm{II}}| > 10^{-12}$; and in 80-digit arithmetic on 480 points, namely $h = i/400$, $h = 10^{-k/4}$ and $h = 1-10^{-k/4}$ for $1 \le i \le 400$ and $1 \le k \le 40$. This is numerical verification, not a proof. For the real-coefficient formulas B_3 and B_4 the coefficients $Q_0, \ldots, Q_4$ are determined by the matching conditions, given the outer constants and δ (Section 8); the values in Appendix B reproduce them to the 16 printed digits, which suffices in double precision, but exact agreement with the series through h^4 (and hence the comparison with R_{II} as $e \to 0$) requires computing them from the matching conditions. Likewise, all constants of S_3 and S_4 are determined by the matching conditions, and their very small errors for moderate eccentricities (Section 9 and Table 3) were computed with constants accurate to 70 digits; with the 16-digit constants of Appendix B, rounding of the constants limits these errors to between about 10^{-22} near the circle and 10^{-18} at $e = 0.9$, which is still far below double-precision resolution.

15. Concluding remarks

The main results of this note are the closed formulas A_3, A_4 and A_6. A few AGM steps written as one expression are accurate for all but very flat ellipses. Legendre's relation rewrites the remaining case exactly in terms of K and two power series in b/a; truncating the series and estimating K from the same AGM steps gives an expression that is a short polynomial in b/a apart from the estimate of K, and one extra term makes the result continuous. With three, four and six square roots and no loops, this gives formulas whose errors in exact arithmetic lie below the unit roundoff of single, double and quadruple precision for every eccentricity, including the degenerate ellipse, and which are accurate to within about six units of the unit roundoff when evaluated in that precision (for A_6, as estimated with 34-digit decimal arithmetic). The errors of A_4 and A_6 are many orders of magnitude smaller than those of recent closed formulas [23, 4, 5], the most accurate of which has a maximum error of 4.5×10^{-10}. Proposition 4.1 shows that the construction is not limited to these three cases: for every switch point, enough AGM steps and series terms give a continuous formula of this kind with any prescribed maximum error, and the error of the continuous formula is at most that of the AGM branch plus twice that of the flat-ellipse branch. Such formulas need only arithmetic operations and square roots and the same few coefficients for every shape, without piecewise coefficient tables, and have no fitted parameters: apart from the integers N and n, small integers in the refined estimate of K, and the series coefficients, which are dyadic rationals (for A_3, A_4 and A_6 exactly representable even in binary32), they contain only a freely chosen switch point and a continuity coefficient given by the closed formula (18), which need not be stored to many digits. In our latency model, A_4 is faster in double precision than the quadruple-nested formulas and, for flat ellipses ($b/a < 0.09$), than an AGM loop iterated to the same accuracy, whose cost grows without bound as $b \to 0$; in

single precision A_3 is the cheapest way we found to reach nearly full precision. Approximations that use a logarithm, such as Cody's Chebyshev approximations of E [13], can be faster still.

The nested-radical formulas complement these results. Ramanujan's second approximation owes its high order of agreement with the Gauss–Kummer series to the vanishing of two coefficients in the ideal radicand (6), and nesting further square roots is a natural way to continue his construction. With integer coefficients, two more radicals reduce the maximum error by more than two orders of magnitude while keeping the formula short enough to write down. With real coefficients and four radicals, the maximum error drops to 8.98×10^{-9} for formulas that are nowhere less accurate than R_{II} and to 3.90×10^{-9} for minimax formulas. Within the same number of square roots, the choice between series matching and minimax optimisation is a choice between accuracy for nearly circular ellipses and uniform accuracy. In our latency model these formulas are slower than the main formulas of comparable or better accuracy, but they remain single expressions without branches and with fewer operations, which matters when throughput rather than latency limits the speed. Evaluated in powers of $\sigma = 1 - h$, they are also accurate in single precision, where the triple-nested C_3 is as fast as five AGM steps, beyond which the binary32 AGM does not improve (2.0×10^{-6} for $b/a \geq 10^{-6}$), and about ten times more accurate.

Provenance statement

The results in this note were obtained with the assistance of Claude Opus 5.5 (Anthropic), working under the direction of the author. The model derived the AGM-based formulas and Proposition 4.1 with its proof, carried out the series computations behind Propositions 6.1 and 6.2, the searches for integer and real-coefficient formulas, the optimisations, the high-precision verification and the cost estimates, produced the figures, drafted the text and checked the references. The computations were done in Python, in exact rational arithmetic, in arbitrary-precision decimal arithmetic with up to 110 digits, and in native or exactly emulated binary32 and binary64 floating-point arithmetic. The author is responsible for the content.

References

[1] M. Abramowitz and I. A. Stegun (eds.), *Handbook of Mathematical Functions*, Nat. Bur. Standards Appl. Math. Ser. 55, Washington, 1964.

[2] S. Adlaj, *An eloquent formula for the perimeter of an ellipse*, Notices Amer. Math. Soc. **59** (2012), no. 8, 1094–1099. doi:10.1090/noti879

[3] G. Almkvist and B. C. Berndt, *Gauss, Landen, Ramanujan, the arithmetic-geometric mean, ellipses, π, and the Ladies Diary*, Amer. Math. Monthly **95** (1988), no. 7, 585–608. doi:10.2307/2323302

[4] S. E. Ayala-Raggi and M. Rendón-Marín, *Is simplicity still possible for a more accurate approximation to the perimeter of the ellipse? or, Using the exponential function to further improve the second Ramanujan's approximation*, preprint arXiv:2510.16191, 2025.

[5] S. E. Ayala-Raggi and M. Rendón-Marín, *Approximating the ellipse perimeter by "bending the line": the ELIP closed-form family*, preprint arXiv:2610.28689, 2026.

[6] G. A. Baker, Jr. and P. Graves-Morris, *Padé Approximants*, 2nd ed., Encyclopedia Math. Appl. 59, Cambridge University Press, Cambridge, 1996.

[7] R. W. Barnard, K. Pearce and L. Schovanec, *Inequalities for the perimeter of an ellipse*, J. Math. Anal. Appl. **260** (2001), no. 2, 295–306. doi:10.1006/jmaa.2000.7128

[8] J. M. Borwein and P. B. Borwein, *Pi and the AGM: A Study in Analytic Number Theory and Computational Complexity*, Wiley, New York, 1987.

[9] R. P. Brent, *Fast multiple-precision evaluation of elementary functions*, J. ACM **23** (1976), no. 2, 242–251. doi:10.1145/321941.321944

[10] B. C. Carlson, *Numerical computation of real or complex elliptic integrals*, Numer. Algorithms **10** (1995), no. 1, 13–26. doi:10.1007/BF02198293

[11] B. C. Carlson, *Elliptic integrals*, Chapter 19 of the *NIST Digital Library of Mathematical Functions*, https://dlmf.nist.gov/19.

[12] S. Chowla and A. Selberg, *On Epstein's zeta-function*, J. Reine Angew. Math. **227** (1967), 86–110. doi:10.1515/crll.1967.227.86

[13] W. J. Cody, *Chebyshev approximations for the complete elliptic integrals K and E*, Math. Comp. **19** (1965), no. 89, 105–112; Corrigendum, ibid. **20** (1966), no. 93, 207. doi:10.1090/S0025-5718-1965-0171370-4

[14] A. Fog, *Instruction tables: Lists of instruction latencies, throughputs and micro-operation breakdowns for Intel, AMD and VIA CPUs*, Technical University of Denmark, https://www.agner.org/optimize/.

[15] T. Fukushima, *Fast computation of complete elliptic integrals and Jacobian elliptic functions*, Celest. Mech. Dyn. Astron. **105** (2009), 305–328. doi:10.1007/s10569-009-9228-z
[16] T. Fukushima, *Precise and fast computation of the general complete elliptic integral of the second kind*, Math. Comp. **80** (2011), no. 275, 1725–1743. doi:10.1090/S0025-5718-2011-02455-5
[17] T. Fukushima, *Precise and fast computation of complete elliptic integrals by piecewise minimax rational function approximation*, J. Comput. Appl. Math. **282** (2015), 71–76. doi:10.1016/j.cam.2014.12.038
[18] C. Hastings, Jr., *Approximations for Digital Computers*, Princeton University Press, Princeton, 1955.
[19] *IEEE Standard for Floating-Point Arithmetic*, IEEE Std 754-2019, 2019. doi:10.1109/IEEESTD.2019.8766229
[20] J. Ivory, *A new series for the rectification of the ellipsis; together with some observations on the evolution of the formula* $(a^2 + b^2 - 2ab\cos\theta)^n$, Trans. Roy. Soc. Edinburgh **4** (1798), 177–190. doi:10.1017/S0080456800030817
[21] Th. Kaluza, *Über die Koeffizienten reziproker Potenzreihen*, Math. Z. **28** (1928), 161–170. doi:10.1007/BF01181155
[22] E. E. Kummer, *Über die hypergeometrische Reihe*, J. Reine Angew. Math. **15** (1836), 39–83 and 127–172. doi:10.1515/crll.1836.15.39, doi:10.1515/crll.1836.15.127
[23] P. Moscato and A. Ciezak, *A new approximation for the perimeter of an ellipse*, Algorithms **17** (2024), no. 10, 464. doi:10.3390/a17100464
[24] M. J. D. Powell, *Approximation Theory and Methods*, Cambridge University Press, Cambridge, 1981.
[25] S. Ramanujan, *Modular equations and approximations to* π, Quart. J. Pure Appl. Math. **45** (1914), 350–372.
[26] E. Salamin, *Computation of* π *using arithmetic-geometric mean*, Math. Comp. **30** (1976), no. 135, 565–570. doi:10.2307/2005327
[27] U. Shankar, *Perimeter of an ellipse: understanding Ramanujan's approximation*, preprint arXiv:2603.03373, 2026.
[28] M. Parker (Stand-up Maths), *Why is there no equation for the perimeter of an ellipse?*, YouTube video, 5 September 2020, https://www.youtube.com/watch?v=5nW3nJhBHL0.
[29] S. Sýkora, *Approximations of ellipse perimeters and of the complete elliptic integral* $E(x)$*: review of known formulae*, Stan's Library, Vol. I, 2005. doi:10.3247/SL1Math05.004
[30] S. Sýkora, *Advances in approximations of ellipse perimeters and of the complete elliptic integral*, Stan's Library, Vol. II, 2007.
[31] M. B. Villarino, *Ramanujan's perimeter of an ellipse*, preprint arXiv:math/0506384, 2005.

Appendix A. Proof of Proposition 4.1

By homogeneity we may assume $a = 1$. Then $t = b \in [0,1]$ and $k = \sqrt{1-t^2}$, and we write $\widetilde{E}(t) = E(k) = P/4$ and $\widetilde{K}(t) = K(k) = \pi/(2M(1,t))$; note that $1 \le \widetilde{E} \le \pi/2$. Let $F_N = P_N/4$, let $\widehat{K}_N$ be the estimate of K, and let $G_{N,n} = \widehat{K}_N\mathcal{P}_n + \mathcal{Q}_n = P^{\mathrm{L}}_{N,n}/4$ and $A = A_{N,n}/4$.

Part (a). The AGM quantities a_j and b_j are continuous functions of $t \in [0,1]$, and $a_{j+1} \ge a_j/2$ gives $a_N + b_N \ge a_N \ge 2^{-N} > 0$. Hence $\widehat{K}_N$ and $G_{N,n}$ are continuous on $[0,1]$, and F_N is continuous on $(0,1]$. The two branches agree at $t = t_s$ by the choice of γ, so A is continuous. At $t = 0$ we have $\mathcal{P}_n(0) = 0$ and $\mathcal{Q}_n(0) = 1$, so $A(0) = 1$, that is, $P = 4a$. At $t = 1$ all a_j and b_j equal 1 and $c_1 = 0$, so $F_N(1) = \pi/2$, that is, $P = 2\pi a$.

Step 1: the AGM. For $0 < t \le 1$ the AGM started from $(1,t)$ satisfies $b_j \le b_{j+1} \le M \le a_{j+1} \le a_j$, where $M = M(1,t)$. Hence $a_N + b_N = 2a_{N+1} \ge 2M$, $a_{j+1} - b_{j+1} \le (a_j - b_j)/2 \le 2^{-j-1}$, and

$$a_{j+1} - b_{j+1} = \frac{(a_j - b_j)^2}{2(\sqrt{a_j} + \sqrt{b_j})^2} \le \frac{(a_j - b_j)^2}{8t}.$$

For $\delta \le t \le 1$ with $\delta > 0$ the convergence is therefore uniform, and eventually doubly exponential: once $a_j - b_j < 8\delta$, the quantity $(a_j - b_j)/(8\delta)$ is at least squared in every step. Since $2M \ge 2\delta$ and $|a_N + b_N - 2M| \le a_N - b_N$, both estimates of K converge to $\widetilde{K} = \pi/(2M)$, and F_N converges to $\widetilde{E}$, because the tail $\sum_{j>N} 2^{j-1}c_j^2$ of (7), with $c_j = (a_{j-1} - b_{j-1})/2$, tends to zero; all of this holds uniformly for $\delta \le t \le 1$. Moreover, $a_N + b_N \ge 2M$ gives $0 \le \pi/(a_N + b_N) \le \widetilde{K}$, and $3a_N^2 + 10a_Nb_N + 3b_N^2 \ge 3(a_N + b_N)^2$ shows that the estimate (16) lies between 0 and $\frac{4}{3}\widetilde{K}$. For both estimates, therefore,

$$|\widehat{K}_N(t) - \widetilde{K}(t)| \le \widetilde{K}(t) \qquad (0 < t \le 1). \tag{26}$$

Step 2: the series. Let $w_n = \big((\frac{1}{2})_n/n!\big)^2$, $f(m) = \sum_{n\ge0} w_n m^n$ and $g(m) = \sum_{n\ge0} w_n m^n/(1-2n)$. Then $K(t) = \frac{\pi}{2}f(t^2)$ and $E(t) = \frac{\pi}{2}g(t^2)$ for the modulus t, so $\mathcal{Q}(t) = 1/f(t^2)$ and $\mathcal{P}(t) =$

$1-g(t^2)/f(t^2)$. The ratio $w_{n+1}/w_n = \big((2n+1)/(2n+2)\big)^2$ increases with n, so the sequence (w_n) is log-convex. By Kaluza's theorem [21], the power series of $1/f$ has the form $1-\sum_{n\ge1}\beta_n m^n$ with all $\beta_n \ge 0$. For every N, the recursion that defines the β_n shows that the product of $f(m)$ with the truncation $1-\sum_{n=1}^{N}\beta_n m^n$ equals 1 plus a power series with nonnegative coefficients (the coefficient of m^k, $k>N$, is $\sum_{i<k-N} w_i\beta_{k-i}$). Since $f>0$ on $[0,1)$, this gives $\sum_{n=1}^{N}\beta_n m^n < 1$ for $0\le m<1$, and letting $m\to1$ and then $N\to\infty$ gives $\sum_{n\ge1}\beta_n \le 1$. In particular the series of $1/f$ converges absolutely for $|m|\le1$ and represents $1/f$ for $|m|<1$. The coefficients of g are absolutely summable as well, with sum of absolute values $2-2/\pi$. Since absolutely summable sequences are closed under the Cauchy product, the coefficients of $\mathcal{P} = 1-g\cdot(1/f)$ are absolutely summable too. Write $\mathcal{P}(t) = \sum_{j\ge1} p_j t^{2j}$ and $\mathcal{Q}(t) = \sum_{j\ge0} q_j t^{2j}$, and let $C = \sum_{j\ge1}|p_j|$, $\tau_n^{\mathcal{P}} = \sum_{j>n}|p_j|$ and $\tau_n^{\mathcal{Q}} = \sum_{j>n}|q_j|$. Then the series converge uniformly on $[0,1]$, $\tau_n^{\mathcal{P}}, \tau_n^{\mathcal{Q}} \to 0$, and for $0\le t\le1$

$$|\mathcal{P}(t)-\mathcal{P}_n(t)| \le \tau_n^{\mathcal{P}}\, t^{2n+2}, \qquad |\mathcal{Q}(t)-\mathcal{Q}_n(t)| \le \tau_n^{\mathcal{Q}}, \qquad |\mathcal{P}_n(t)| \le C\,t^2. \tag{27}$$

By continuity, Legendre's relation $\widetilde{E} = \widetilde{K}\mathcal{P} + \mathcal{Q}$ holds for $0<t\le1$. (For $t_s<1$, uniform convergence on $[0,t_s]$ suffices, and this follows without Kaluza's theorem whenever $K(t_s)<\pi$, that is, for $t_s<0.984$: then $|f(m)-1|\le f(|m|)-1<1$ for $|m|\le t_s^2$, so f has no zeros there.)

Step 3: the growth of K. By Legendre's relation, $\widetilde{K}\mathcal{P} = \widetilde{E}-\mathcal{Q} \to 1-1 = 0$ as $t\to0$. The function $\mathcal{P}(t)/t^2$ is continuous on $(0,1]$, tends to $p_1=\frac12$ as $t\to0$, and is positive, because $E(t)<K(t)$ for $0<t<1$ and $\mathcal{P}(1)=1$. Its infimum c on $(0,1]$ is therefore positive, and $t^2\widetilde{K}(t) \le (\widetilde{E}-\mathcal{Q})/c$. Consequently

$$\eta(\delta) = \sup_{0<t\le\delta} t^2\widetilde{K}(t) \to 0 \quad (\delta\to0), \qquad \kappa = \sup_{0<t\le1} t^2\widetilde{K}(t) < \infty.$$

Step 4: the error bound. For $0<t\le t_s$, Legendre's relation gives

$$G_{N,n} - \widetilde{E} = (\widehat{K}_N - \widetilde{K})\,\mathcal{P}_n + \widetilde{K}\,(\mathcal{P}_n - \mathcal{P}) + (\mathcal{Q}_n - \mathcal{Q}).$$

By (27), the last two terms are bounded by $\kappa\tau_n^{\mathcal{P}}$ and $\tau_n^{\mathcal{Q}}$. The first is bounded by $Ct^2|\widehat{K}_N-\widetilde{K}|$, which by (26) is at most $C\eta(\delta)$ for $t\le\delta$, and at most $C\omega_N(\delta)$ with $\omega_N(\delta) = \sup_{\delta\le t\le1}|\widehat{K}_N-\widetilde{K}|$ for $t\ge\delta$. At $t=0$, $G_{N,n}=\widetilde{E}=1$. Hence

$$\Lambda = \max_{0\le t\le t_s}|G_{N,n}-\widetilde{E}| \le C\big(\eta(\delta)+\omega_N(\delta)\big) + \kappa\tau_n^{\mathcal{P}} + \tau_n^{\mathcal{Q}}.$$

Let $\varphi_N = \max_{t_s\le t\le1}|F_N-\widetilde{E}|$. The continuity coefficient satisfies

$$|\gamma|\,t_s^{2n+2} = |F_N(t_s)-G_{N,n}(t_s)| \le \varphi_N + \Lambda,$$

so $|\gamma t^{2n+2}| \le \varphi_N+\Lambda$ for $t<t_s$, and

$$\max_{0\le t\le1}|A-\widetilde{E}| \le \max\big(\varphi_N,\, 2\Lambda+\varphi_N\big) = \varphi_N + 2\Lambda,$$

which is part (b). Given $\varepsilon>0$, choose δ with $2C\eta(\delta)<\varepsilon/4$; then n_0 with $2(\kappa\tau_n^{\mathcal{P}}+\tau_n^{\mathcal{Q}})<\varepsilon/4$ for all $n\ge n_0$; and finally N_0 with $\varphi_N<\varepsilon/4$ and $2C\omega_N(\delta)<\varepsilon/4$ for all $N\ge N_0$, using Step 1 with δ and with t_s. Then $|A-\widetilde{E}|<\varepsilon$ on $[0,1]$, and since $\widetilde{E}\ge1$, also $|A/\widetilde{E}-1|<\varepsilon$. This proves part (c). □

Appendix B. Constants of the real-coefficient formulas

All formulas have the form (19), $P \approx \pi(a+b)\big(1+3h/(q+\sqrt{r_1+\sqrt{\cdots+\sqrt{Q(h)}}})\big)$ with $Q(h) = \sum_k Q_k h^k$. The constants are given to between 11 and 16 significant digits, mostly 15 or 16. The number of digits actually needed is discussed in Section 6.5: in powers of h the quadruple-nested formulas need up to 14 of them, in powers of σ at most 11. The very small errors near the circle reported for B_3, B_4, S_3 and S_4 require more digits of the matched coefficients (Section 14). Tables 6 and 7 give the coefficients Q_k of the innermost polynomial in powers of h, and Table 8 gives the coefficients g_k of the same polynomial in powers of $\sigma = 1-h = 4ab/(a+b)^2$, which should be used in floating-point evaluation. The two sets are separate roundings of the same

polynomials. Since $g_0 = Q(1)$ is much smaller than the Q_k for the deeper formulas, the g_k computed from the rounded Q_k differ from those in Table 8 in the last digits, and for B_4 and C_4 already in the ninth significant digit of g_0 (relative differences 7×10^{-10} and 6×10^{-8}); the coefficients in powers of σ should therefore be taken from Table 8.

The double-nested formulas B_2 and S_2 are the members $c^* = 1.6083816339$ and $c = \frac{3}{2}(\sqrt{17}-3)$ of the family (20). The formula C_2 has $q = 10.0090857908803$, $r_1 = 0.6128422340926082$ and $Q(h) = 11.21355851685472 - 19.93701722530456h + 8.831504042401445h^2$, or in powers of $\sigma = 1 - h$, $Q = 0.108045333951605 + 2.27400914050167\sigma + 8.831504042401445\sigma^2$.

TABLE 6. Constants of the real-coefficient triple-nested formulas (innermost polynomial in powers of h).

	B_3	S_3	C_3
q	10.29433900484506	9.901118545551911	7.019352275714195
r_1	−3.341141176193871	−15.32081840331176	13.80578502232042
r_2	13.28678013650547	245.7056780801806	2.351193196498491
Q_0	664.6588071841899	20567.63325898943	14080.40649434002
Q_1	−1649.12127158747	−35626.48944268275	−38989.58516019706
Q_2	1413.808679491932	17956.04055956124	35812.57137464874
Q_3	−486.7455903150188	−2257.517954692982	−10847.28729948503
Q_4	58.91906584057077	47.95933656661023	−54.74049119699177

TABLE 7. Constants of the quadruple-nested formulas (innermost polynomial in powers of h).

	B_4	S_4	C_4
q	10.85467560067979	6.398229749134604	10.86740281549944
r_1	−14.99617978628396	7.724819030181588	−12.95175980740153
r_2	217.4248221484751	81.68388870382054	165.6816448386081
r_3	60.69690320044219	3430.148049356863	5.370651452451673
Q_0	5262043.703342058	50595750312.388	1847512.118262919
Q_1	−24948584.87807319	−170923436563.0533	−9715172.366338652
Q_2	48781397.45217162	225198491690.7474	21117013.89003979
Q_3	−50145829.27576912	−145074484755.0125	−24214491.83091987
Q_4	28369626.76334429	46568798796.73117	15460171.06217302
Q_5	−8303793.301070271	−6601332084.471917	−5410777.648048259
Q_6	1070262.324933209	264381866.3523564	1152269.946706327
Q_7	−122188.4721802651	1598629.223142381	−316369.8247714597
Q_8	37070.28010040734	62156.11535253739	79844.77403337315

TABLE 8. Coefficients of the innermost polynomial in powers of $\sigma = 1 - h = 4ab/(a+b)^2$, $Q = \sum_k g_k \sigma^k$, for the real-coefficient triple- and quadruple-nested formulas; the outer constants q and r_j are those of Tables 6 and 7.

	B_3	S_3	C_3
g_0	1.519690614203828	687.6257577415486	1.36491810967023
g_1	46.06442018637908	6295.124841372778	125.2662741426501
g_2	307.0863035903005	11471.24271488195	2942.26652901169
g_3	251.0693269527357	2065.680608426541	11066.249264273
g_4	58.91906584057077	47.95933656661023	−54.74049119699177

	B_4	S_4	C_4
g_0	4.596798741646269	29830049.01970314	0.12113718121
g_1	920.3678708487985	883393830.4320084	34.97146318858
g_2	49681.99525125551	7375548941.57889	2724.84316439066
g_3	500669.5751169605	19465540320.49015	37821.6497160375
g_4	1222918.212710306	17588169320.54159	206522.3378616636
g_5	2372241.581633772	4977988930.212046	669616.9421420527
g_6	1252910.862482759	277312642.1442241	1173334.846240557
g_7	−174373.7686229936	−2095878.14596268	−322388.3674955255
g_8	37070.28010040734	62156.11535253739	79844.77403337315